Lithos 112 (2009) 289–305

Contents lists available at ScienceDirect

Lithos

journal homepage: www.elsevier.com/locate/lithos

Geochemical and zircon U–Pb and Hf isotopic study of the Baijuhuajian metaluminous A-type granite: Extension at 125–100 Ma and its tectonic significance for South China

Jean Wong [a], Min Sun [a,*], Guangfu Xing [b], Xian-hua Li [c,d], Guochun Zhao [a], Kenny Wong [a], Chao Yuan [c], Xiaoping Xia [a], Longming Li [a], Fuyuan Wu [d]

[a] Department of Earth Sciences, The University of Hong Kong, Hong Kong SAR, China
[b] Institute of Geology and Mineral Resources, Nanjing, China
[c] Key Laboratory of Isotope Geochronology and Geochemistry, Guangzhou Institute of Geochemistry, Chinese Academy of Sciences, Guangzhou 510640, China
[d] State Key Laboratory of Lithospheric Evolution, Institute of Geology and Geophysics, Chinese Academy of Sciences, P.O. Box 9825, Beijing 100029, China

ARTICLE INFO

Article history:
Received 11 December 2008
Accepted 5 March 2009
Available online 21 March 2009

Keywords:
A-type granite
Mesozoic
South China
Zircon U–Pb age
Hf isotope

ABSTRACT

The Early Cretaceous Baijuhuajian pluton is an A-type granitic intrusion, emplaced along the Jiangshan-Shaoxing (JSSX) fault zone in western Zhejiang Province, SE South China. It intruded into a Late Jurassic volcanic basin bounded by Proterozoic sandstone and siltstone. The granite has a coarse-grained, porphyritic texture and is composed of alkali feldspar phenocrysts in a matrix of K-feldspar, quartz, plagioclase and biotite. The pluton has a clear A-type geochemical signature, e.g. it is metaluminous (A/CNK ~ 1.0) and has high SiO_2 (75 to 78 wt.%), total alkalis ($Na_2O + K_2O = 4.8$ to 8.5 wt.%), rare earth elements (total REE = 228 to 438 ppm), HFSE and Fe* [$FeO_t/(FeO_t + MgO) = 0.87$ to 0.97]. On the other hand, it is characterized by low CaO (0.51 to 1.01 wt.%), TiO_2 (0.06 to 0.13 wt.%), P_2O_5 (below detection) and Sr (7.0 to 9.5 ppm). The hypersolvus texture and fine-grained groundmass indicate emplacement at a shallow-depth. SHRIMP U–Pb zircon dating yielded a weighted mean $^{206}Pb/^{238}U$ age of 126 ± 3 Ma and zircons from this pluton give $\varepsilon Hf(T)$ values between −0.52 and +4.24, suggesting the importance of juvenile material in the magma source.
Most of the plutonic rocks in southeast China are calc-alkaline, subduction-related intrusions of Jurassic and Cretaceous age. Previous studies suggested that the sparse A-type granites in South China were emplaced in two episodes: 190–155 Ma in the inland area and ~100 Ma along the coastal area in SE South China. Our study of the Baijuhuajian granite, together with the coeval Suzhou A-type granite (123 Ma) in Jiangsu Province, defines an important extensional event between 125 and 100 Ma. Considering the available data for the Mesozoic igneous rocks in South China, we suggest that subduction of the Pacific plate in the Mesozoic produced voluminous calc-alkaline granitoids and volcanic rocks with a younging trend from west to east. The A-type granites were generated during periods of local extension at 190–155 Ma and 125–100 Ma, perhaps corresponding to localized rollback of the Pacific plate.

1. Introduction

Tectonic evolution of the South China Craton during the Mesozoic is a hot topic and has been intensively studied for more than half a century. The geology of the eastern South China is characterized by a wide Mesozoic magmatic belt. The intense magmatic activity in the region mainly occurred in two episodes, one in the Jurassic (Early Yanshanian, 180–142 Ma) and one in the Cretaceous (Late Yanshanian, 142–67 Ma) (e.g. Li, 2000; Zhou and Li, 2000). The magmatic rocks show an oceanward younging trend, i.e. those in the western inland area are Jurassic whereas those in the eastern coastal area are Cretaceous (Li et al., 2007b; Zhou et al., 2006). The Jurassic igneous rocks are predominantly fractionated I-type granites with very limited A-type granites and basaltic volcanic rocks (e.g. Li et al., 2007a; Li, 2000). In contrast, rocks of the Cretaceous episode are dominated by high-potassium I- and a few A-type granites (e.g. Li, 2000; Zhou et al., 2006).

The evolution of magmatic compositions in southeastern China is usually attributed to the subduction of the paleo-Pacific plate beneath the Eurasian plate (e.g. Charvet et al., 1994; Holloway, 1982; Martin et al., 1994). Generation of I-type granites in the Jurassic is usually considered to correspond to the subduction environment, whereas the development of A-type granites in the Cretaceous may indicate an extensional environment (e.g. Charvet et al., 1994; Jahn et al., 1976; Lapierre et al., 1997; Martin et al., 1994). This magmatic belt in SE China is much wider than that normally observed in subduction zones (>1000 km), and some authors argue that the presence of Mesozoic

* Corresponding author. Tel.: +852 2859 2194.
E-mail address: minsun@hku.hk (M. Sun).

0024-4937/$ – see front matter © 2009 Elsevier B.V. All rights reserved.
doi:10.1016/j.lithos.2009.03.009

wrench faults (e.g. Xu et al., 1987), rift systems (e.g. Gilder et al., 1991) and extensional or rift basins (e.g. Chen and Dickinson, 1986) in eastern China is not compatible with the subduction model (e.g. Li, 2000). Hence, the timing and cause of the extension are key issues for understanding the tectonic evolution of this region. Some workers consider that extension started in the Jurassic (e.g. Gilder et al., 1991; Li, 2000), based on the emplacement of subordinate rift-related alkaline basalts and syenites (e.g. Wang et al., 2004), bimodal volcanic and intrusive rocks (Chen et al., 1999b; Wang et al., 2005) and mafic dykes in the southeastern China hinterland (Li and McCulloch, 1998). Other researchers argue that extension in southeastern South China began in the Cretaceous (e.g. Charvet et al., 1994; Lapierre et al., 1997; Martin et al., 1994) as A-type granites and bimodal volcanic rocks were mainly emplaced at ~100 Ma in the coastal region.

It is apparent that petrogenetic characteristics of the igneous rocks need to be studied in much greater detail in order to understand the tectonic evolution of the South China Craton in the Mesozoic. The A-type granites and coeval mafic rocks are particularly important because they may indicate an extensional tectonic environment on a local or regional scale (e.g. Eby, 1992; Turner et al., 1992; Whalen et al., 1987), and can give information about the magma source and tectonic regime in the southeastern China during Mesozoic.

This paper concerns a newly discovered A-type granitic pluton in Baijuhuajian, western Zhejiang Province. Field investigations, petrographic and geochemical studies, zircon U–Pb and Hf isotope analyses, and whole rock Sr–Nd isotope analyses were carried out. Using these new data, we review and discuss the significance of the Mesozoic A-type granites in the magmatic belt in order to better understand the Mesozoic magmatic evolution of the region.

2. Geological background

The South China Craton is surrounded by the North China Craton in the north, the Tibetan Plateau in the west, the Indochina Block in the southwest and the Philippine Sea Plate in the east. The Craton itself is composed of the Yangtze Block in the northwest and the Cathaysia Block in the southeast. The basement of the Yangtze Block consists of Archean to Proterozoic rocks exposed in the western regions, such as Kongling, Kangding, and Dahongshan areas (e.g. Ames et al., 1996; Qiu et al., 2000b; Zheng et al., 2006; Greentree and Li, 2008). Recent studies on xenocrystic zircons from Early Paleozoic lamproite diatremes give 2.9–2.8 Ga U–Pb ages and 2.6–3.5 Ga Hf model ages (Zheng et al., 2006), and the authors suggested that an Archean basement is possibly widely distributed in the Yangtze Block. On the other hand, the Cathaysia Block may have a widespread Proterozoic basement (e.g. Chen and Jahn, 1998; Xu et al., 2007).

Timing of the amalgamation between the Yangtze and Cathaysia Blocks is considered at ~1.1 Ga to 0.9 Ga (e.g. Chen and Jahn, 1998; Li et al., 2007c; Ye et al., 2007) or later based on a younger, ca. 866 Ma K–Ar age of glaucophanes from a blueschist in the suture zone (Zhao and Cawood, 1999). The southeastern margin of the South China Craton used to be considered as a passive margin until the Early Mesozoic, when the paleo-Pacific Plate was subducted under the eastern flank of the South China Craton (e.g. Hsü et al., 1990). Recent studies on the Wuzhishan orthogneiss in Hainan Island suggest that the southeastern margin of the South China Craton may have changed from a passive to an active continental margin as early as the Early Permian (Li et al., 2006). Massive and vigorous magmatic activity occurred in the southeastern China from the Permo-Triassic to Late Cretaceous in three episodes; Indosinian

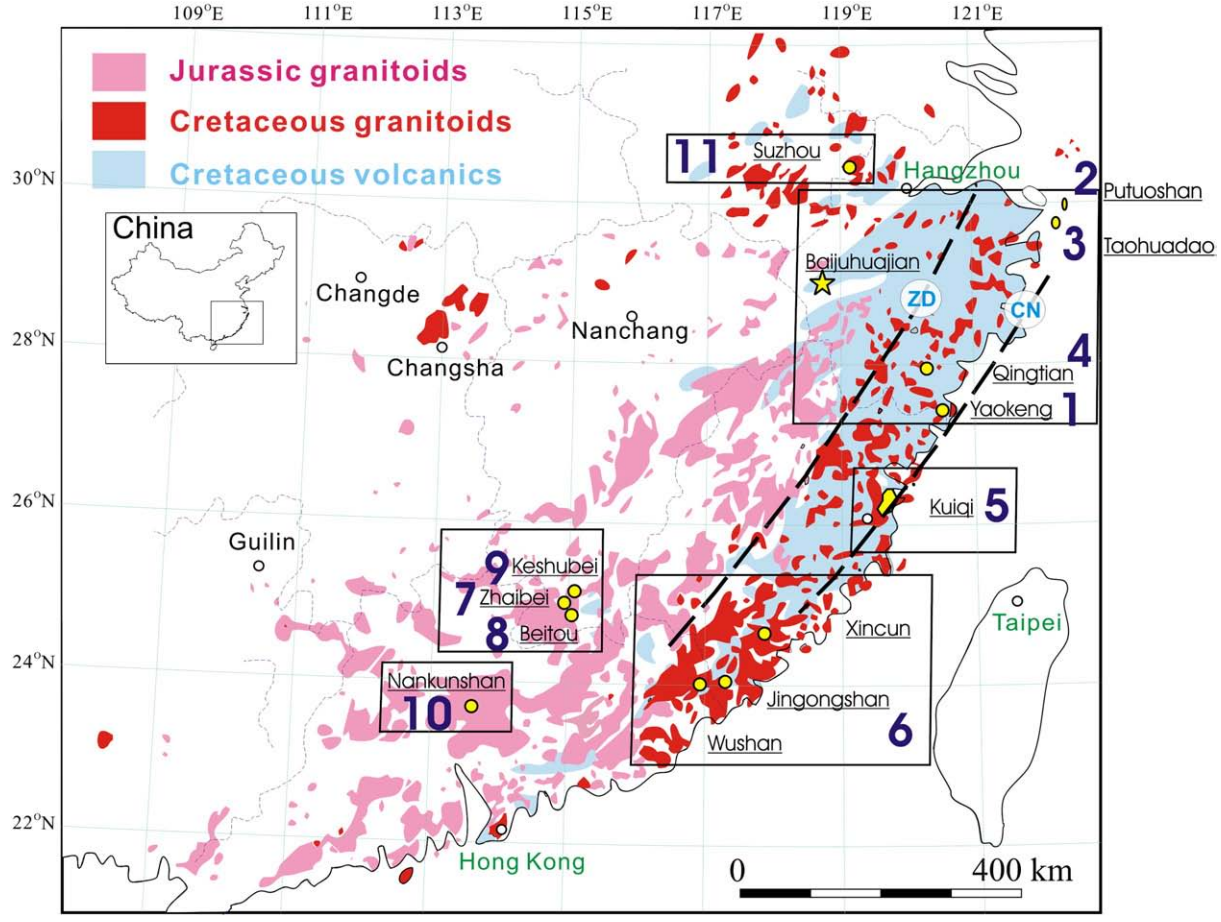

Fig. 1. Distribution of the Yanshanian magmatic rocks in southeastern South China showing representative Mesozoic A-type granites (marked by yellow circles) (modified after Zhou et al., 2006). The yellow star indicates the locality of the Baijuhuajian A-type granite. Two fault zones are marked by dashed lines: ZD = Zhenghe-Dapu fault and CN = Changle-Nan'ao fault. (For interpretation of the references to color in this figure legend, the reader is referred to the web version of this article.)

Table 1
List of representative A-type granites in the Mesozoic magmatic belt, southeastern South China.

No.	Location	Lithology	Age (Ma)	Dating method	Reference
	Zhejiang Province				
1	Yaokeng (YK)	Alkaline granite	116 ± 6	Rb–Sr whole rock	Qiu et al. (2000a)
2	Putuoshan (PTS)	Alkaline granite	93.6 ± 0.4	U–Pb zircon	Qiu et al. (1999)
3	Taohuadao (THD)	Alkaline granite	92.9 ± 0.6	U–Pb zircon	Qiu et al. (1999)
4	Qingtian (QT)	Alkaline granite	101.2 ± 2	U–Pb zircon	Qiu et al. (1999)
	Fujian Province				
5	Kuiqi (KQ)	Peralkaline granite	93 ± 1	Rb–Sr whole rock	Martin et al. (1994)
6	Wushan (WS) –	Alkaline granite	95	Assigned in the literature, based on the similar pluton in the region	Qiu et al. (2000b)
	Jingangshan (JGS) –	Alkaline granite	92 ± 3	Rb–Sr whole rock	Qiu et al. (2000b)
	Xincun (XC)	Alkaline granite	97.12 ± 2.32	Rb–Sr whole rock	Qiu et al. (2000b)
	Jiangxi Province				
7	Zhaibei (ZB)	Biotite K-fsp Granites	176 ± 10	Rb–Sr whole rock	Chen et al. (1998)
			171.6 ± 4.6	SHRIMP U–Pb zircon	Liu et al. (2003)
8	Beitou (BT)	K-fsp Granites	178 ± 0.84	Rb–Sr whole rock	Fan and Chen (2000)
9	Keshubei (KSB)	Biotite Granites	189 ± 3	SHRIMP U–Pb zircon	Li et al. (2007a)
	Guangdong Province				
10	Nankunshan (NKS)	Aluminous A-type granite	158 ± 5	SHRIMP U–Pb zircon	Li et al. (2007b)
	Jiangsu Province				
11	Suzhou (SZ)	Alkaline granites	123.4 ± 0.8	Ar–Ar (biotite) dating	Chen et al. (1993)

granitoids (265 to 205 Ma), Early Yanshanian granitoid-volcanic rocks (180 to 142 Ma) and Late Yanshanian granitoid-volcanic rocks (140 to 66 Ma) (Zhou et al., 2006). The granitoids include I-, S- and A-type granites, and the A-type granites generally occur along regional and local fault zones in southeastern China (Fig. 1 and Table 1). Most of the A-type granites were emplaced along the coastal region during the Late Yanshanian stage (ca. 100 Ma) (e.g. Wang et al., 2005). For example, the Kuiqi, Wushan, Jingangshan and Xincun A-type granites in Fujian and Yaokeng, Putuo, Taohuadao and Qingtian A-type granites in Zhejiang were emplaced along the Changle-Nan'ao fault zone (e.g. Martin et al., 1994; Qiu et al., 1999), and similarly, the distribution of Zhaibei, Beitou and Keshubei A-type granites are constrained by the Shannan-Xunwu fault in Jiangxi (e.g. Chen et al., 1998, 1999c; Hu et al., 2002) and the Suzhou A-type granite was emplaced at the intersection of the NE-striking Mudu syncline tension fault and the NW-striking fault in Jiangsu (Zhang et al., 1988). Basaltic rocks or rhyolites are locally associated with the A-type granites.

The genetic relationship between the A-type granites and I-type granitoids is variable. For example, the Kuiqi alkaline granite (93 Ma) postdates the subduction-related Danyang monzogranite (103 Ma) and the Fuzhou syenogranite (104 Ma); the Nankunshan aluminous A-type granite (158 Ma) is associated with the Fogang I-type granite (159 to 165 Ma) within the Fogang-Fengshun and Yuanping-Xinfeng faults (Bao and Zhao, 2003). These examples indicate that a time gap of 10 my or less existed between emplacement of the I- and A-type granites. The contrasting magmatic series at Kuiqu versus Danyang and Fuzhou was attributed to reactivation of a deep crustal fault due to the change in the tectonic settings (Martin et al., 1994). On the other hand, the Fogang I-type granite and Nankunshan A-type granite in the southern Jiangxi Province were both interpreted to be related to upwelling of the asthenospheric mantle and mafic magma intra-/under-plating due to the break-up of flat-slab subduction in the Early Jurassic (~190 Ma) and subsequent slab foundering in the middle Jurassic (Li et al., 2007b). The previously proposed tectonic models envisage the occurrence of A-type granites as due to a change in tectonic setting from subduction to extension (e.g. Martin et al., 1994; Zhou et al., 2006), or as result of a change in subduction direction (e.g. Sun et al., 2007) or subduction angle (e.g. Zhou and Li, 2000), which may have been caused by break-up of the subducting slab (e.g. Li and Li, 2007).

We recently identified a new A-type granite, named as the Baijuhuajian pluton, in northeastern Quzhou, western Zhejiang Province, China (Fig. 2). The granite crops out in an area of ~30 km^2, along the northwest of the NW-trending Jiangshan-Shaoxing fault zone (Fig. 2). Regionally, the granite intruded into a volcanic basin filled by the Upper Jurassic Suichang Formation that was developed on Proterozoic to Carboniferous sedimentary strata (refer to the 1:200,000 geological map, BGMRZP, 1989). The associated volcanic rocks include porphyritic rhyolite, silicic tuff and ignimbrites (BGMRZP, 1989). A reconnaissance zircon U–Pb isotopic study of the Baijuhuajian pluton by the local mapping team gave an age of 137 Ma, but the details of the analytical method and results were not reported (BGMRZP, 1989). The Baijuhuajian pluton and the volcanic rocks were assigned a middle Yanshanian age by BGMRZP (1989), equivalent to the Valanginian stage within the Early Cretaceous epoch according to the most recent geological time scale (Ogg et al., 2008).

3. Field investigations

The Baijuhuajian pluton intruded into Proterozoic (Sinian) sedimentary strata on the west and the 'Upper Jurassic' Huangjian and Laochun Formations on the southeast (refer to the 1:200,000 geological map, BGMRZP, 1989). Although the pluton crops out over an extensive area, it is heavily vegetated. Samples collected for this study were exposed in a new road cut and are generally fresh, where the Baijuhuajian pluton intruded the fine-grained pyroclastic rocks of the 'Upper Jurassic' Huangjian and Laochun Formations (Fig. 3a and b). A sharp contact, without a significant chilled margin, was observed between the pluton and the volcanic rocks. In the field, the outcrops of Baijuhuajian pluton are grey on fresh surfaces, turning yellowish-grey when weathered. The pluton has a porphyritic texture with alkali feldspar phenocrysts ranging from 0.2 to 20 mm in size. The phenocrysts are euhedral to subhedral, pearly white to greyish in colour and are compositionally zoned. Quartz grains are subhedral to anhedral, and occur in the finer-grained matrix (<0.4 mm diameter). The size of the quartz grains decreases as the size of feldspar phenocrysts increases. Biotite is fine-grained (≤0.3 mm) and typically forms small aggregates.

Mafic enclaves, although not abundant, are present in the Baijuhuajian granite. They are small, very fine-grained and highly altered (Fig. 3c and d). Two types of enclaves are recognized; one is dark grey and elongate (ca. 15 cm wide and ca. 45 cm long), whereas the other is dark green and ellipsoidal (various sizes from 0.2 cm to 20 cm). The ellipsoidal enclaves are distributed unevenly in the pluton

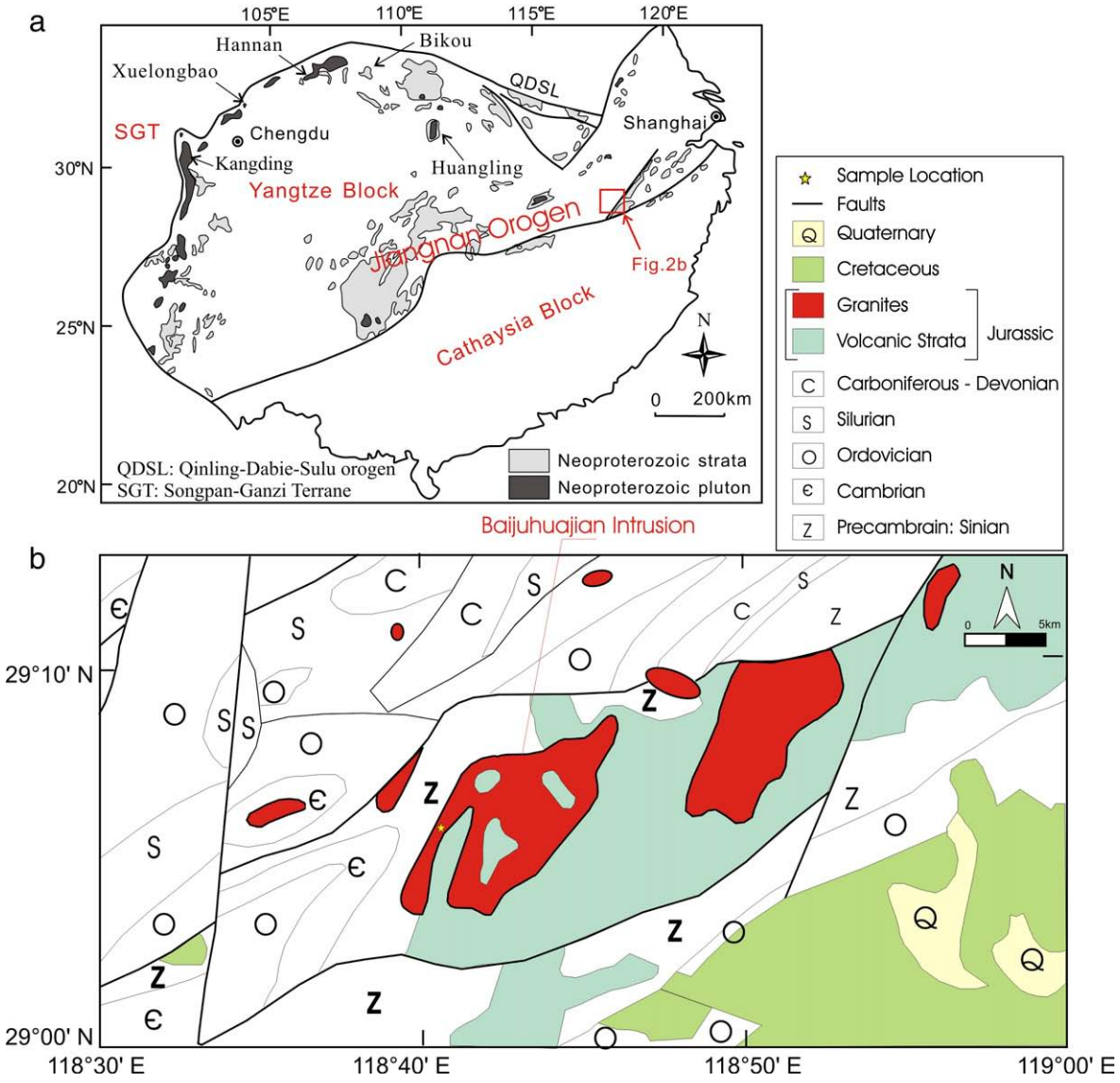

Fig. 2. (a) Regional geological map of China. The South China Craton is composed of the Yangtze Block in the north and the Cathaysia Block in the south (modified after Wang et al., 2006). (b) Geological map of the Baijuhuajian granite in Furong Town, western Zhejiang Province. The pluton was emplaced into the Precambrian sedimentary strata and later cut by local NE–SW-trending faults.

and are composed of minute pyroxene grains and some needle-shaped opaque minerals (1 mm long). Interaction between the granitic magma and the two groups of enclaves can be inferred by the small feldspar and felsic veins formed in the margins of the enclaves and by the presence of small quartz and alkaline feldspar phenocrysts in the enclaves.

Well-developed quartz veins intruded both the granitic host rocks and the mafic xenoliths. It is believed that the quartz veins were generated by late-stage hydrothermal activity. Tourmaline, galena, fluorite and pyrite are the main accessory minerals in the veins.

4. Petrography

Twenty-five samples were collected on the NW side of the Furong Reservoir along a new road across the pluton (Table 2), including 16 samples of granite, 7 of elongated xenoliths, and two of ellipsoid xenoliths. All of the samples were cut for thin sections and the granitic samples were crushed for chemical analyses. The granite samples are light grey to yellowish-gray with fine-grained granophyric textures. The major minerals are alkali feldspar (~40 vol.%), quartz (~42 vol.%), biotite (ca. 8 vol.%) and plagioclase feldspar (ca. 5 vol.%) (Fig. 4a). Opaque minerals, mainly magnetite, occur as accessory minerals. The K-feldspar phenocrysts range up to ~3 mm whereas the groundmass feldspars, are ~1 mm in size. Perthitic textures are pervasive in the granites. Small amounts of sericite locally replace the feldspars. Quartz is subhedral to anhedral, ranging from 3 to <1 mm. All of the granites have granophyric textures (Fig. 4b), indicating rapid cooling and high level emplacement. Fragmentation of alkali feldspar phenocrysts increases towards the margins of the pluton.

The elongate xenoliths contain small plagioclase phenocrysts in a groundmass of sericite, amphibole, ilmenite and Fe oxides. The small ellipsoidal enclaves also contain ~20 vol.% Fe oxide minerals (magnetite and hematite). Apatite makes up <2 vol.% of the small ellipsoidal xenoliths and ~9 vol.% of the elongate xenoliths.

5. Analytical methods

5.1. Major and trace elemental analyses

Major and trace elemental analyses were carried out in the Department of Earth Sciences, The University of Hong Kong. Major oxide concentrations were determined by wavelength-dispersive X-

Fig. 3. (a) The Baijuhuajian granitoid (left) intruded into the Late Jurassic volcanic strata (on the right). (b) Porphyritic texture of the Baijuhuajian granite. Phenocrysts are alkali feldspar and the groundmass consists of alkali feldspar, quartz and biotite. (c) Large, dark grey, elongate xenoliths (ca. 15 cm wide and ca. 45 cm long). (d) Dark green, ellipsoidal enclaves (0.5 mm up to 12×20 cm) with a very fine-grained texture. (For interpretation of the references to color in this figure legend, the reader is referred to the web version of this article.)

ray fluorescence spectrometry (XRF) on fused glass beads using a Philips PW 2400 spectrometer with matrix correction following a procedure described by Norrish and Hutton (1969). BHVO-2 (basalt), JGB-2 (gabbro), G2 and G3 (granites), and a Chinese national rock standard GSR-1 (granite) were used as reference materials. The accuracies of the XRF analyses are estimated to be ca. 1% (relative) for SiO_2 and ca. 2% (relative) for the other oxides.

Trace-element compositions were analyzed by inductively coupled plasma mass spectrometry (ICP-MS) of nebulized solutions using a VG Plasma-Quad Excell ICP-MS at The University of Hong Kong. The detailed analytical procedures are described by Qi et al. (2000). About 50±1 mg of powdered sample were digested in Teflon bombs using mixed HF and HNO_3. ^{103}Rh was used as an internal standard solution to monitor drift (Qi et al., 2000). Two multi-element standard solutions, one containing Li, Ba, V, Cr, Co, Ni, Cu, Zn, Ga, Rb, Sr, Cs, Ba, Pb, Th, U, Sc, Y and fourteen REEs and the other containing W, Mo, Nb, Ta, Zr, and Hf, were employed for external calibration. The reference standards were the same as those used for the XRF analyses. The accuracies for most of the trace elements are estimated to be better than ca. 5% (relative). Geochemical data are presented in Table 3 for major oxides and Table 4 for trace elements.

5.2. Sr–Nd isotopic analyses

Whole rock Rb–Sr and Sm–Nd isotope compositions were determined for a representative granite sample (06ZFR01). It was analyzed using a Finnigan MAT 262 thermal ionization mass spectrometer (TIMS) at the Institute of Geology and Geophysics, Chinese Academy of Sciences, Beijing, China following procedures described by Wei et al. (2004). About 50 mg of whole rock powdered sample was dissolved in a Teflon bomb using a mixture of HF and HNO_3. Sr and rare earth elements (REE) were isolated using a 0.2-ml column filled with Sr-Spec and RE-Spec resins (manufactured by Eichrom Industries, Inc.), for selective extraction of Sr and REE, respectively. Nd fractions were further separated and purified using LN resin with HCl as eluent. Procedures for performing mass analyses followed those described by Qiao (1988).

Measured $^{87}Sr/^{86}Sr$ and $^{143}Nd/^{144}Nd$ ratios were normalized against the natural $^{86}Sr/^{88}Sr$ ratio of 0.1194 and $^{146}Nd/^{144}Nd$ ratio of 0.7219, respectively. The reported $^{87}Sr/^{86}Sr$ ratio was adjusted to the

Table 2
List of samples collected from the Baijuhuajian pluton with locations and lithology.

Sample No	Lithology
N 29° 06′ 36.4″	*E 118° 38′ 53.4″*
06ZFR-01	Granite
06ZFR-02	Granite
06ZFR-03	Elongate xenolith A
06ZFR-03-1	Elongate xenolith A
06ZFR-03-2	Elongate xenolith A
06ZFR-03-3	Elongate xenolith A
N 29° 06′ 28.5″	*E 118° 39′ 10.1″*
06ZFR-08	Granite
06ZFR-09	Ellipsoid enclave 1
N 29° 06′ 36.4″	*E 118° 38′ 53.4″*
07ZFR-01	Granite
07ZFR-02	Granite
07ZFR-03	Granite
07ZFR-05	Granite
07ZFR-04	Granite
N 29° 06′ 50.8″	*E 118° 38′ 49.0″*
07ZFR-06	Granite
N 29° 06′ 45.3″	*E 118° 38′ 49.0″*
07ZFR-07	Granite
07ZFR-08	Granite
07ZFR-09	Granite
N 29° 06′ 44.8″	*E 118° 38′ 49.3″*
07ZFR-10	Granite
07ZFR-11	Granite
N 29° 06′ 44.0″	*E 118° 38′ 49.4″*
07ZFR-12	Granite
07ZFR-13	Granite
07ZFR-17	Ellipsoid enclave 2
N 29° 06′ 40.7″	*E 118° 38′ 52.3″*
07ZFR-21	Elongate xenolith B
07ZFR-23	Elongate xenolith B
07ZFR-24	Elongate xenolith B

measured NBS SRM 987 standard of 0.710226 ± 12 (2σ), whereas the reported $^{143}Nd/^{144}Nd$ ratio was adjusted to the measured JMC and Ames Nd standards of 0.511937 ± 7 (2σ) and 0.512124 ± 8 (2σ). Concentrations of Rb, Sr, Sm and Nd were determined using ICP-MS in the Department of Earth Sciences, The University of Hong Kong. The initial $^{87}Sr/^{86}Sr$ and $^{143}Nd/^{144}Nd$ ratios were calculated based on the SHRIMP U–Pb zircon age obtained in this study. The results are presented in Table 5.

5.3. Zircon U–Pb and Hf isotopic compositions

Individual zircon grains were separated from a representative granitic sample (06ZFR08) by heavy-liquid and magnetic methods followed by hand picking under a binocular microscope. Representative grains were mounted on adhesive tape, enclosed in epoxy resin and polished to about half their thickness. The transmitted and reflected light images of the grains were photographed, and cathodoluminescence (CL) images of the zircons were taken using a Mono CL3 detector (manufactured by Gatan, U.S.A.) attached to an Electron Microprobe (manufactured by JXA-8100, JEOL, Japan) at the Guangzhou Institute of Geochemistry, Chinese Academy of Sciences, Guangzhou, China for investigating the structure and morphology of the zircons and selecting spots for U–Pb dating and Lu–Hf analysis.

5.3.1. SHRIMP U–Pb dating

U–Th–Pb analyses were carried out using the WA consortium SHRIMP II ion microprobe housed at the Curtin University of Technology, Perth, Australia whose instrumental performance and analytical procedures are documented by Nelson (1997). The sample mounts were cleaned and gold-coated and measurements of U, Th and Pb were made on the exposed zircon surfaces. Fragments of the Sri Lankan gem zircon standard CZ3 (Pidgeon et al., 1994) were incorporated in each mount as reference to monitor the isotopic ratios, using $^{206}Pb/^{238}U$ ratio of 0.09143 equivalent to an age of 564 Ma. Pb/U ratios of the unknown samples were corrected using the ln(Pb/U)/ln(UO/U) relationship as measured in the standard CZ3. The U and Th decay constants recommended by Steiger and Jäger (1977) were used to calculate the ages of the samples. All reported ages calculated using $^{207}Pb/^{206}Pb$ data were corrected against measured ^{204}Pb. The analytical data were then reduced, calculated and plotted using the Squid 1.0 and IsoplotEx 3.0 programs (Ludwig, 2003). Detailed analytical data in which individual analyses are shown with 1σ error and uncertainties in weighted mean ages quoted at the 95% confidence level (2σ) are given in Table 6.

5.3.2. Lu–Hf isotope analysis

Hf isotopic analyses were preformed using an ArF excimer laser ablation system, attached to a Neptune Plasma multi-collector ICP-MS at the Institute of Geology and Geophysics, Chinese Academy of Sciences, Beijing, China. Hf isotopic data reported in this study were obtained from the zircon grains with U–Pb data, with a beam diameter of 32 μm, pulse rate of 8 Hz and energy density of 15 J/cm^2. Detailed analytical procedures are described by Wu et al. (2006). Each analytical spot was subjected to 200 ablation cycles, resulting in pits 20–40 μm deep. Atomic masses 172, 173, 175 to 180 and 182 were simultaneously measured in static-collection mode. Isobaric interference of ^{176}Yb on ^{176}Hf was

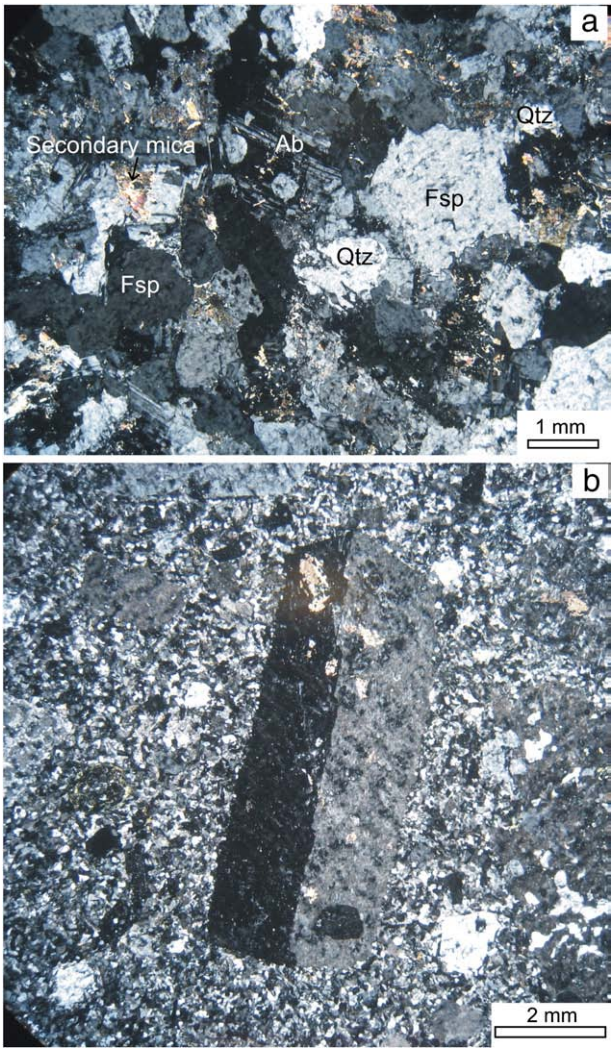

Fig. 4. (a) Mineral assemblage of the Baijuhuajian granite, consisting of alkali feldspar, quartz, biotite and secondary mica. Sample 06ZFR01, crossed polars, 4×. (b) Granophyric texture of the Baijuhuajian granitoid indicates rapid cooling and shallow-level emplacement. Sample 06ZFR08, crossed polars, 4×.

Table 3
Major element data for the Baijuhuajian granite (in wt.%).

Sample no.	SiO_2	Al_2O_3	TiO_2	Fe_2O_3*	MnO	MgO	CaO	Na_2O	K_2O	P_2O_5	L.O.I.	Total
06ZFR01	76.19	11.53	0.06	2.83	0.12	0.10	0.56	2.36	3.85	0.00	1.43	99.02
06ZFR02	75.24	12.44	0.13	1.89	0.03	0.11	1.01	3.04	5.03	0.00	0.90	99.82
06ZFR08	76.92	11.64	0.10	1.22	0.04	0.06	0.55	3.99	4.07	n.d.	0.80	99.39
07ZFR01	76.20	11.70	0.12	1.44	0.02	0.12	0.65	3.65	4.23	n.d.	0.77	98.90
07ZFR02	76.64	11.75	0.11	1.33	0.02	0.11	0.53	3.89	4.04	n.d.	0.83	99.25
07ZFR03	77.30	11.95	0.11	1.35	0.02	0.10	0.57	3.87	3.97	n.d.	0.67	99.91
07ZFR04	77.25	12.37	0.07	0.55	0.01	0.07	0.51	3.50	5.02	n.d.	0.55	99.89
07ZFR05	77.13	11.98	0.10	1.24	0.02	0.11	0.59	3.45	4.58	n.d.	0.72	99.92
07ZFR06	76.88	12.03	0.10	0.94	0.01	0.07	0.54	3.70	4.61	n.d.	0.70	99.58
07ZFR07	77.13	11.85	0.10	1.36	0.02	0.09	0.55	3.61	4.26	n.d.	0.77	99.73
07ZFR08	77.07	12.11	0.10	1.43	0.02	0.09	0.56	3.50	4.36	n.d.	0.77	99.99
07ZFR09	76.65	11.81	0.12	1.57	0.02	0.09	0.56	3.50	4.22	n.d.	0.90	99.44
07ZFR10	77.65	11.50	0.10	0.78	0.02	0.05	0.56	3.99	4.24	n.d.	0.73	99.63
07ZFR11	77.32	11.47	0.09	1.14	0.04	0.06	0.56	3.69	4.29	n.d.	0.80	99.46
07ZFR12	76.90	12.04	0.10	1.08	0.01	0.07	0.53	3.78	4.40	n.d.	0.80	99.71
07ZFR13	76.61	12.17	0.10	1.09	0.01	0.07	0.54	3.64	4.53	n.d.	0.67	99.43

L.O.I. = loss on ignition. n.d. for not detected. Fe_2O_3* = Total Fe oxides represented in form of Fe_2O_3.

corrected against the $^{176}Yb/^{172}Yb$ ratio of 0.5886 (Chu et al., 2002). Interference of ^{176}Lu on ^{176}Hf was corrected by measuring the intensity of the interference-free ^{175}Lu isotope and using a recommended $^{176}Lu/^{175}Lu$ ratio of 0.02655 (Machado and Simonetti, 2001). External calibration was made by measuring zircon standard 91500 with the unknowns during the analyses to evaluate the reliability of the analytical data, which yielded a weighted mean $^{176}Hf/^{177}Hf$ ratio of 0.282366 ± 39 ($n = 21$).

Calculation of the initial $^{176}Hf/^{177}Hf$ ratios was done using the measured $^{176}Lu/^{177}Hf$ ratios and the ^{176}Lu decay constant of 1.865×10^{-11} yr^{-1} reported by Scherer et al. (2001). εHf values were calculated using the chondritic $^{176}Hf/^{177}Hf$ values of 0.282772 and $^{176}Lu/^{177}Hf$ of 0.0332 reported by Blichert-Toft and Albarede (1997). Assuming that the depleted mantle reservoir has a linear isotopic growth from $^{176}Hf/^{177}Hf = 0.279718$ at 4.55 Ga to 0.283250 at present, with a $^{176}Lu/^{177}Hf$ value of 0.0384 (Griffin et al., 2004), the depleted mantle Hf model ages (T_{DM}) were calculated using the measured $^{176}Lu/^{177}Hf$ ratios of zircon. The mantle extraction model age (T^c_{DM}) was calculated by projecting initial $^{176}Hf/^{177}Hf$ ratios of the zircon to the depleted mantle model growth line using mean $^{176}Lu/^{177}Hf$ value (0.015) for average continental

Table 4
Trace-element data for the Baijuhuajian granite.

	06ZFR01	06ZFR02	06ZFR08	07ZFR01	07ZFR02	07ZFR03	07ZFR04	07ZFR05	07ZFR06	07ZFR07	07ZFR08	07ZFR09	07ZFR10	07ZFR11	07ZFR12	07ZFR13
Trace element (ppm)																
Ga	39.2	23.9	27.6	26.4	29.8	25.2	20.1	26.8	23.8	25.0	23.7	25.0	20.9	21.6	25.3	22.2
Rb	580	900	315	899	869	834	1010	1010	1210	1070	1080	1050	1070	997	1090	1080
Sr	8.17	9.22	38.8	9.46	9.11	8.25	7.36	9.35	8.11	7.41	7.06	6.96	7.48	7.75	8.13	7.87
Y	130	97.3	147	138	115	98.5	97.3	123	90.4	87.7	79.5	94.3	85.5	103	96.1	80.8
Zr	127	155	231	230	167	167	166	186	168	161	173	183	180	181	173	151
Nb	93.1	93.6	60.5	112	91.1	93.8	75.9	87.2	84.3	87.0	84.2	95.6	94.0	85.4	91.1	92.1
Ba	101	16.5	133	17.5	20.7	17.6	35.1	16.1	21.0	21.7	19.2	21.8	19.3	20.6	27.3	22.7
La	40.2	43.6	76.8	53.8	45.0	46.2	45.5	48.3	42.5	44.7	41.2	42.4	42.9	43.7	38.9	37.0
Ce	92.7	102	166	126	102	108	108	110	101	102	95.3	99.7	99.5	97.8	86.5	86.7
Pr	11.0	11.2	20.5	14.6	11.5	12.1	11.9	12.5	11.2	11.4	10.7	10.9	10.2	10.5	10.4	9.26
Nd	36.8	39.0	73.4	53.7	41.2	44.2	42.1	46.6	39.6	41.2	38.8	40.2	36.0	38.9	37.7	34.0
Sm	10.8	9.51	18.7	13.7	10.7	10.7	9.83	11.7	9.82	10.0	9.45	10.1	8.47	9.45	9.51	8.56
Eu	0.06	0.07	0.46	0.10	0.08	0.07	0.08	0.09	0.08	0.08	0.07	0.07	0.06	0.07	0.08	0.07
Gd	10.3	9.56	17.0	13.8	10.5	10.8	9.76	12.0	9.87	9.78	9.15	9.70	8.72	9.68	9.50	8.60
Tb	2.28	2.00	3.19	3.10	2.34	2.34	2.09	2.58	2.07	2.08	1.91	2.11	1.78	2.12	2.10	1.87
Dy	17.2	14.6	22.5	22.2	16.7	16.0	15.0	18.3	14.5	14.7	13.3	15.4	13.1	14.9	15.7	13.5
Ho	3.94	3.51	4.99	5.20	3.91	3.67	3.65	4.25	3.28	3.38	3.06	3.59	3.06	3.68	3.68	3.11
Er	13.9	10.9	15.1	16.5	13.1	11.8	11.7	14.0	10.2	10.2	9.60	11.0	9.66	11.3	11.3	9.75
Tm	2.56	2.05	2.45	3.07	2.51	2.22	2.17	2.62	1.92	1.86	1.64	2.06	1.78	2.12	2.17	1.83
Yb	17.3	14.2	14.4	20.7	17.4	14.9	14.9	17.4	12.8	13.0	11.2	13.8	12.1	14.2	14.5	12.2
Lu	2.66	2.09	2.11	3.07	2.55	2.11	2.18	2.55	1.96	1.95	1.75	1.97	1.78	2.01	2.09	1.85
Hf	7.23	8.69	9.41	14.4	10.3	9.62	9.97	11.9	9.64	9.34	9.68	10.4	10.1	10.5	9.74	8.84
Ta	11.8	20.7	4.45	19.1	19.6	17.2	19.5	15.7	15.9	15.6	15.2	17.6	19.4	17.1	16.3	17.3
Th	45.3	47.4	33.1	78.5	52.1	56.4	53.3	59.7	55.3	57.5	51.8	53.8	52.8	53.1	53.3	48.8
U	18.7	19.6	8.96	28.2	19.3	22.3	22.9	22.0	23.1	24.1	23.3	22.2	23.1	22.8	19.9	19.9
Zr + Nb + Y + Ce	443	448	604	606	475	467	447	506	443	437	432	472	459	467	447	410
Eu/Eu*	0.02	0.02	0.08	0.02	0.02	0.02	0.02	0.02	0.02	0.02	0.02	0.02	0.02	0.02	0.03	0.03
La_N	169	184	324	227	190	195	192	204	179	189	174	179	181	185	164	156
Yb_N	101	83.8	84.7	122	102	87.9	87.5	102	75.5	76.4	66.1	81.3	70.9	83.4	85.3	71.7
REE	261	264	438	349	279	285	279	303	261	266	247	263	249	260	244	228
LREE/HREE	2.73	3.49	4.37	2.99	3.05	3.46	3.54	3.11	3.61	3.68	3.79	3.41	3.80	3.34	3.00	3.33

Eu/Eu* is a measure of the europium anomaly when compare to Sm and Gd. $Eu/Eu^* = Eu_N/\sqrt{[(Sm_N).(Gd_N)]}$.

Table 5
Results of Sr–Nd isotopic analyses of the Baijuhuajian granitoid (06ZFR01).

Sample no.	Lithology	Rb (ppm)	Sr (ppm)	$^{87}Rb/^{86}Sr$	$^{87}Sr/^{86}Sr$	(2σ)	$^{87}Sr/^{86}Sr(i)$	Sm (ppm)	Nd (ppm)	$^{147}Sm/^{144}Nd$	$^{143}Nd/^{144}Nd$	(2σ)	$^{143}Nd/^{144}Nd$ (i)	$\varepsilon_{Nd}(t)$	T_{DM} (Ma)
06ZFR01	Granite	434	7.85	156	1.0699	13	0.7917	9.89	40.5	0.153467	0.512472	14	0.51235	−2.55	1488.5

Notes: $\varepsilon_{Nd}(t)$ was calculated based on modern $(^{143}Nd/^{144}Nd)_{CHUR}=0.512638$ and $(^{147}Sm/^{144}Nd)_{CHUR}=0.1967$ (Goldstein et al., 1984). T_{DM} was calculated using present-day $(^{147}Sm/^{144}Nd)_{DM}=0.2137$ and $(^{143}Nd/^{144}Nd)_{DM}=0.51315$ (Peucat et al., 1988). Initial isotopic values were calculated based on the SHRIMP U–Pb zircon age of this study (125.6 Ma).

crust (Griffin et al., 2002). The discussion in this study is based on T^{C}_{DM}. Hf isotope results are reported with a 2σ error in Table 7.

6. Results

6.1. SHRIMP U–Pb zircon geochronology

Representative zircon CL images of the Baijuhuajian granite are shown in Fig. 5a. The zircons chosen for this study are euhedral and prismatic (100 to 150 μm long), with length-to-width ratios of 2:1 to 3:1. Most of them are transparent and colourless under the optical microscope, although some appear brownish due to high U contents. Concentric zoning is common and no inherited cores were observed. A total of 12 zircons were analyzed and the SHRIMP analytical data are presented in Table 6. These zircons have highly variable Th (92 to 996 ppm) and U (161 to 1945 ppm), but their Th/U ratios are quite consistent, ranging from 0.42 to 0.60 (except for one sample with a higher value of 1.02), indicating a magmatic origin (Fig. 5b). All analyses are concordant or nearly concordant and cluster as a single population with a weighted mean $^{206}Pb/^{238}U$ age of 126±3 Ma (MSWD=0.32), which represents the crystallization age of the pluton and was used for the calculation of initial isotopic ratios of the other isotopic systems (Fig. 6).

Table 6
SHRIMP U–Pb isotope composition for the Baijuhuajian granite (06ZFR08).

Spot	U (ppm)	Th (ppm)	Th/U	$^{206}Pb^*$ (ppm)	$^{206}Pb_c$ (%)	$^{207}Pb^*/^{206}Pb^*$	±%	Isotopic ratios				Ages	
								$^{207}Pb^*/^{235}U$	±%	$^{206}Pb^*/^{238}U$	±%	$^{206}Pb^*/^{238}Pb^*$	
FR08-01	161	92	0.59	2.81	0.08	0.0524	5.6	0.1470	6.2	0.0203	2.7	129.8	±3.4
FR08-02	412	190	0.48	6.90	0.40	0.0481	3.6	0.1289	4.4	0.0195	2.5	124.2	±3.1
FR08-03	313	183	0.60	5.36	0.21	0.0477	5.7	0.1312	6.3	0.0199	2.6	127.2	±3.3
FR08-04	406	209	0.53	6.49	0.31	0.0520	4.2	0.1338	5.6	0.0187	3.7	119.3	±4.4
FR08-05	933	438	0.48	16.0	0.09	0.0482	2.9	0.1326	3.8	0.0200	2.5	127.3	±3.1
FR08-06	1324	550	0.43	23.5	1.15	0.0476	4.1	0.1339	4.7	0.0204	2.2	130.2	±2.8
FR08-07	300	141	0.49	4.88	1.10	0.0487	13	0.1260	14	0.0187	2.4	119.7	±2.8
FR08-08	213	103	0.50	3.68	2.33	0.0417	22	0.1130	22	0.0196	2.8	125.4	±3.5
FR08-09	1007	996	1.02	17.2	0.58	0.0486	4.7	0.1327	5.2	0.0198	2.2	126.3	±2.8
FR08-10	412	169	0.42	6.84	0.83	0.0485	7.0	0.1283	7.3	0.0192	2.3	122.5	±2.8
FR08-11	1945	829	0.44	34.2	0.68	0.0493	3.0	0.1383	3.7	0.0204	2.2	129.9	±2.8
FR08-12	356	194	0.56	6.05	1.77	0.0500	15	0.1340	15	0.0194	2.4	124.0	±3.0

Note: Errors are 1σ. Pb_c and Pb* represent the common and radiogenic lead portions, respectively. Common Pb corrected using measured ^{204}Pb.

Table 7
Lu–Hf isotope data for zircons from the Baijuhuajian granitic sample (06ZFR08).

Spot	$^{176}Yb/^{177}Hf$	$^{176}Lu/^{177}Hf$	$^{176}Hf/^{177}Hf$	± (2σ)	$(^{176}Hf/^{177}Hf)_i$	ε_{Hf}	± (1σ)	T_{DM} (Ma)	± (1σ)	T^{C}_{DM} (Ma)
FR08 01	0.104581	0.002438	0.282753	0.000033	0.282747	1.88	1.1	736.0	48	850.4
FR08 02	0.117152	0.002665	0.282780	0.000035	0.282773	2.80	1.2	701.3	52	805.0
FR08 03	0.082813	0.001942	0.282739	0.000040	0.282734	1.42	1.4	746.4	58	872.7
FR08 04	0.066583	0.001543	0.282721	0.000034	0.282717	0.81	1.2	764.6	49	902.9
FR08 05	0.049981	0.001326	0.282720	0.000044	0.282717	0.82	1.5	760.4	63	902.3
FR08 06	0.047104	0.001145	0.282816	0.000038	0.282814	4.23	1.3	620.4	55	734.5
FR08 07	0.028979	0.000670	0.282789	0.000028	0.282788	3.31	1.0	650.9	39	780.0
FR08 08	0.035236	0.000789	0.282726	0.000032	0.282724	1.07	1.1	741.5	45	890.1
FR08 09	0.122941	0.002718	0.282701	0.000030	0.282695	0.03	1.1	818.0	45	941.0
FR08 10	0.074747	0.001703	0.282773	0.000034	0.282769	2.64	1.2	693.0	49	813.1
FR08 11	0.036118	0.000789	0.282773	0.000036	0.282771	2.74	1.3	675.3	51	808.2
FR08 12	0.138764	0.003224	0.282807	0.000036	0.282800	3.74	1.2	670.5	54	758.8
FR08 13	0.045948	0.001056	0.282697	0.000033	0.282695	0.03	1.1	787.7	46	941.4
FR08 14	0.081153	0.001727	0.282818	0.000031	0.282814	4.24	1.1	627.8	45	734.0
FR08 15	0.082322	0.001775	0.282727	0.000027	0.282723	1.03	0.9	759.6	39	892.1
FR08 16	0.112520	0.002350	0.282708	0.000028	0.282703	0.30	1.0	799.9	40	927.9
FR08 17	0.079073	0.001823	0.282684	0.000034	0.282680	−0.52	1.2	823.7	50	968.1
FR08 18	0.047056	0.001119	0.282694	0.000029	0.282691	−0.11	1.0	794.2	41	948.0
FR08 19	0.061727	0.001586	0.282734	0.000032	0.282730	1.28	1.1	746.5	46	880.0
FR08 20	0.023864	0.000649	0.282764	0.000033	0.282763	2.43	1.2	685.4	47	823.3
FR08 21	0.045528	0.001154	0.282704	0.000029	0.282701	0.25	1.0	780.5	42	930.5
FR08 22	0.082835	0.002023	0.282699	0.000027	0.282694	0.00	0.9	806.3	39	942.8
FR08 23	0.032951	0.000860	0.282716	0.000028	0.282714	0.69	1.0	757.8	40	908.8
FR08 24	0.092357	0.002275	0.282763	0.000032	0.282758	2.25	1.1	717.9	47	832.1

Note: The age (125.6 Ma) used for the calculation of 176Hf/177Hf and Hf for the Hf values is dated by the SHRIMP U–Pb methods.

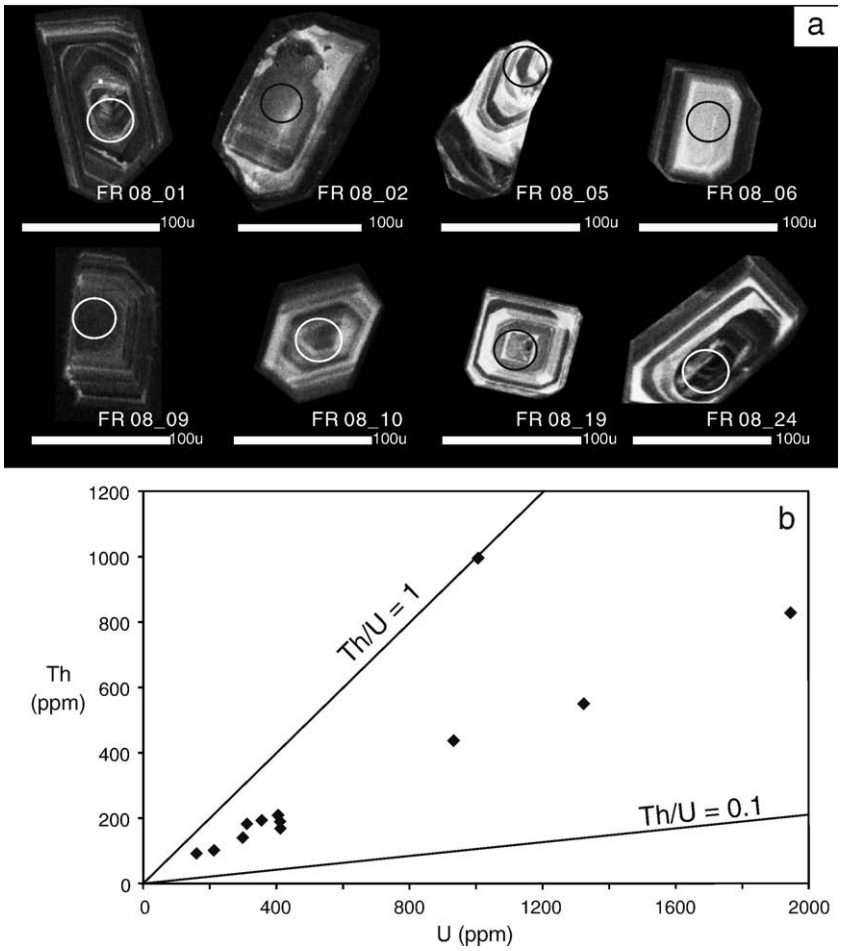

Fig. 5. (a) CL images of representative zircon grains for the Baijuhuajian granite. (b) Th vs U diagram for zircons from the Baijuhuajian granite (06ZFR08). Th/U ratios for the Baijuhuajian granite are between 0.1 and 1, mostly in the range of 0.5 to 0.8.

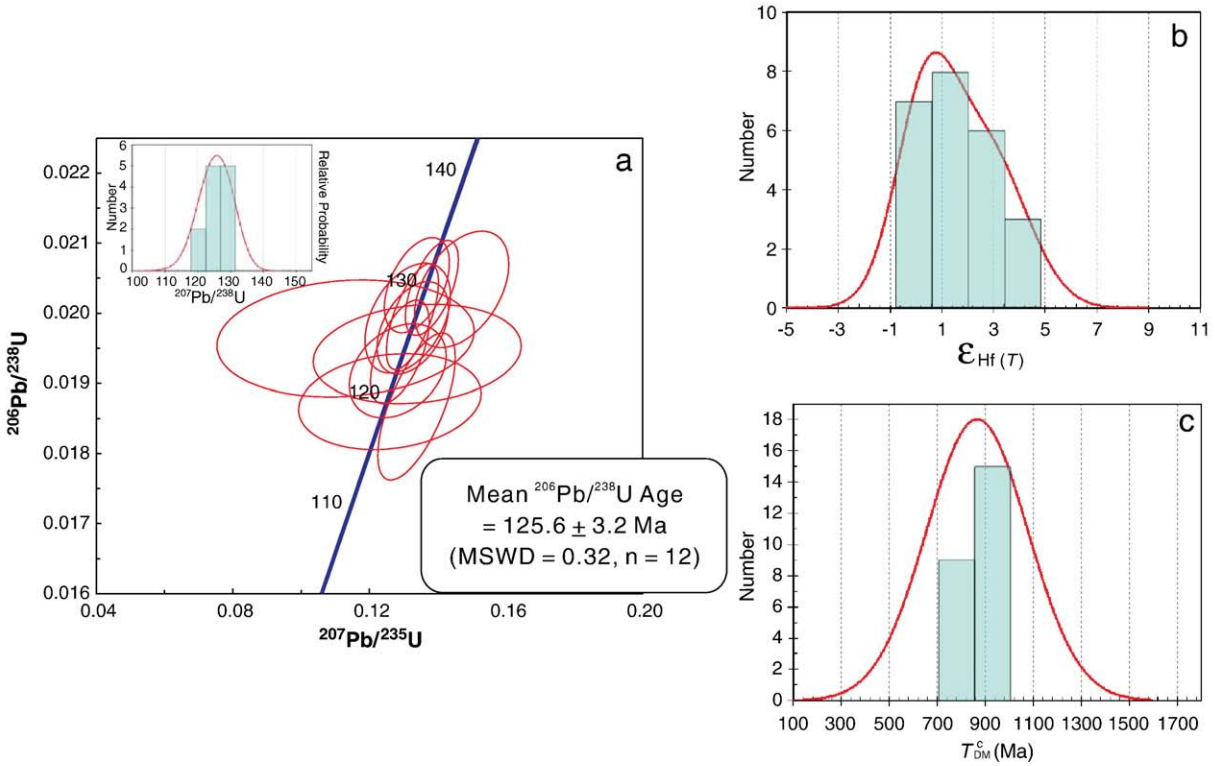

Fig. 6. (a) Concordia diagram of the Baijuhuajian granite (06ZFR08). The weighted mean $^{206}Pb/^{238}U$ age is 125.6 ± 3 Ma. (b) Histograms of $\varepsilon Hf(T)$ and (c) Hf model ages for zircons from the Baijuhuajian granite. Most of the $\varepsilon Hf(T)$ values are positive, ranging from −0.52 to +4.24. The two stage Hf model ages (T_{DM}^{C}) vary from 733 to 968 Ma.

6.2. Major and trace-element geochemistry

A total of 16 granitic samples were analyzed for major and trace-element compositions. The loss on ignition (L.O.I.) for most samples is less than 1 wt.% except for 06ZFR01 which is 1.43 wt.% (Table 3). In general, the granitic samples are characterized by high SiO_2 contents (75.2 to 77.7 wt.%) and have moderate Al_2O_3 contents from 11.5 to 12.4 wt.%. Total iron oxide contents (in the form of Fe_2O_3) vary from 0.55 to 2.83 wt.%. The contents of CaO and Na_2O are 0.51 to 1.01 wt.% and 2.36 to 3.99 wt.%, respectively. The K_2O content ranges from 3.85 to 5.03 wt.%. Other oxides are less than 0.15 wt.%, i.e. MgO = 0.05 to 0.12 wt.%, MnO = 0.01 to 0.12 wt.%, TiO_2 = 0.06 to 0.13 wt.% and P_2O_5 is below the detection limit (<0.001 wt.%).

Element compositions have been recalculated as LOI free for plotting on the geochemical diagrams. According to the Q'-ANOR diagram of Streckeisen and Le Maitre (1979) (Fig. 7a), the samples are classified as syenogranite or alkaline feldspar granite. Most of the samples have ACNK ratios around or greater than 1 (0.95 to 1.27) and possess normative corundum (Al_2O_3) ranging from 0 to 2.51 wt.%, showing a metaluminous or metaluminous-peraluminous character (Fig. 7b). In the K_2O versus SiO_2 diagram of Preccerillo and Taylor (1976) (Fig. 8), the samples fall in the field of the high K, calc-alkaline series. In the Harker diagrams (Fig. 8), Fe_2O_3* and TiO_2 decrease with increasing SiO_2, indicating fractional crystallization of Ti–Fe oxide. No significant correlation can be found for the other oxides due to their low concentrations.

Most of the samples contain less than 10 ppm of Sr (6.9 to 9.5 ppm, except for one with 38.8 ppm). Contents of Nb and Rb are relatively high, ranging from 60.5 to 112 and 315 to 1208 ppm, respectively. The Baijuhuajian pluton exhibits enrichment in REE, with total REE ranging from 228 to 438 ppm. The samples are slightly light REE (LREE)-enriched (La_N/Yb_N = 1.67 to 3.82) with flat heavy REE (HREE) and strong negative Eu-anomalies (Eu/Eu* = 0.02 to 0.08) (Fig. 9a). This indicates removal of plagioclase by crystal fractionation. Decreases in Sr and Ba and slight increases in Rb with increasing SiO_2 may also indicate plagioclase fractionation. Negative anomalies in Ba, Sr, P, Eu and Ti as shown in the primitive mantle-normalized trace-element diagram (Fig. 9b) suggest fractional crystallization of feldspar, apatite and ilmenite. In contrast, Nb, Ta, Zr and Hf are not depleted, implying little contribution of crustal or subduction-related material in the magma source (Fig. 9b).

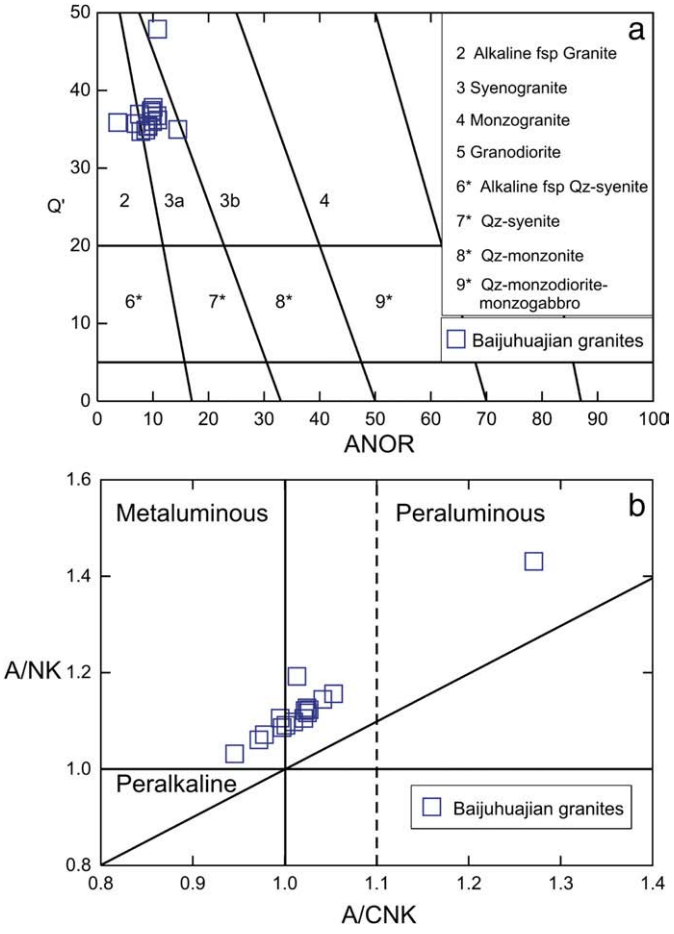

Fig. 7. (a) Rock classification diagram for the Baijuhuajian granite. Samples are classified as syenogranite or alkaline feldspar granite (after Streckeisen and Le Maitre, 1979). (b) A/NK versus A/CNK diagram. The Baijuhuajian granite shows a metaluminous nature. A/NK = Al/(Na + K) (molar ratio). A/CNK = Al/(Ca + Na + K) (molar ratio).

6.3. Whole rock Sr–Nd and zircon Hf Isotopes

The $^{87}Rb/^{86}Sr$ ratio of the Baijuhuajian granite is high (155), giving an unrealistically high I_{Sr} (0.7917) (Table 5). The sample analyzed for Sm–Nd isotope compositions gives a $\varepsilon Nd(T)$ value of −2.55 and a T_{DM} of 1.49 Ga.

Twenty-four zircon grains from the granitic sample 06ZFR08 were analyzed for Hf isotopic compositions (Table 7), yielding $\varepsilon Hf(T)$ values from −0.52 to +4.24 and model ages (T^c_{DM}) from 733 to 968 Ma (Fig. 6b and c). The dominant positive $\varepsilon Hf(T)$ values suggest that juvenile materials played a significant role in the magma generation, consistent with the trace-element data.

7. Petrogenesis and tectonic implications

7.1. The Baijuhuajian pluton: an A-type affinity

The term 'A-type granite' was introduced by Loiselle and Wones (1979) to distinguish a group of granitic rocks that occur in extensional tectonic environments, i.e. rift zones or anorogenic settings. These granites share some common geochemical characteristics, e.g. high Fe/(Fe + Mg) and K_2O/Na_2O ratios, high K_2O contents and enrichment in incompatible elements such as REE (except Eu), Zr, Nb and Ta. A-type granites also have distinctively high TiO_2/MgO ratios (i.e. Douce, 1997). Mafic silicates in this type of granite (if present) have low Co, Sc, Cr, Ni and feldspars have low Ba, Sr and Eu (Loiselle and Wones, 1979). Low water fugacity is common for A-type granites due to anhydrous magmatic conditions.

The Baijuhuajian pluton has all the geochemical characteristics of an A-type granite. The pluton contains moderate to high total alkalis ($K_2O + Na_2O$ = 4.82 to 8.52 wt.%). Its ACNK (0.95 to 1.27) is higher than that of typical I-type granites, showing a metaluminous-peraluminous nature. The pluton has high Fe* values [$FeO_t/(FeO_t + MgO)$ = (0.87 to 0.97)] and low Al_2O_3 contents (less than 12.4 wt.%). The extremely low P_2O_5 abundances and absence of phosphate minerals also suggest that the Baijuhuajian pluton is an A-type granite rather than a S-type leucogranite (Bonin, 2007; King et al., 1997).

The trace-element compositions of the Baijuhuajian granite also show characteristics of A-type granites, e.g. enrichment in HFSE (e.g. Zr, Nb, Y) and REE, and extreme depletion in Ba, Sr, P, Ti and Eu. The pluton has no Nb–Ta anomalies and possesses low La/Nb ratios (0.4–0.6, with one exception in 1.3), which is a prominent feature for A-type granites (La/Nb<1) (Martin et al., 1994). Other trace-element ratios such as Nb/Ta (4–14) and Zr/Hf (16–25) are also consistent with those in typical A-type granites (e.g. Charvet et al., 1994; Eby, 1992; King et al., 1997; Martin et al., 1994).

The extremely low Sr is important in discriminating A-type granites from calc-alkaline granites, as Sr contents in A-type granites are only about 33–50% of those in the calc-alkaline varieties at the same SiO_2 level (Douce, 1997). The Baijuhuajian granites mostly contain <10 ppm Sr, which is significantly lower than typical calc-alkaline I-type granites. Although Y and Nb can be enriched in both A-

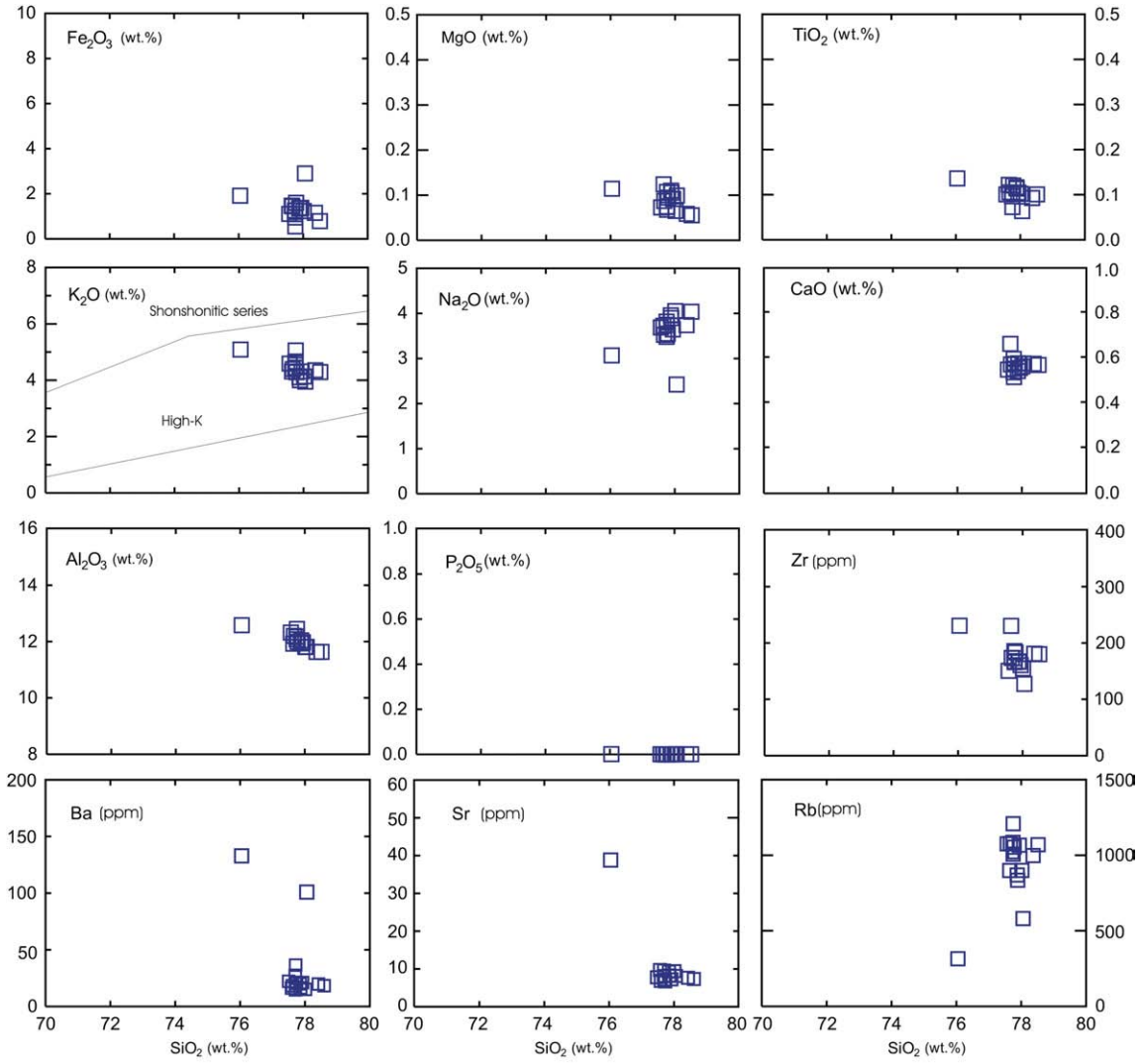

Fig. 8. Harker diagrams for the Baijuhuajian granitic samples.

type and I-type granites, only I-type granites show an Y/Nb fractionation trend (King et al., 1997), a feature conspicuously missing in the Baijuhuajian samples (Fig. 10).

Various discrimination diagrams are also used to constrain the tectonic environment of the Baijuhuajian granite. Samples in this study plot in the field of "within-plate granite" in the diagrams of Pearce et al. (1984) (Fig. 11a) and fall into the field of "A-type granites" in the discrimination diagrams of Whalen et al. (1987), showing its diagnostic geochemical signatures of high FeO_t/MgO ratios (10.5 to 26.4) (Fig. 11b), high Zr, Nb, Ce and Y contents and high $10{,}000 \times Ga/Al$ ratios (>2.7) (Fig. 11c and d).

7.2. Petrogenesis of the Baijuhuajian granite

Although A-type granites are usually associated with extensional tectonic environments, there is no clear consensus on their origin. Models of formation range from fractionation of basaltic magmas, with or without crustal contamination (e.g., Anderson et al., 2003; Loiselle and Wones, 1979; Smith et al., 1999; Turner et al., 1992) to melting of deep crust materials such as granulitic meta-igneous sources that were previously depleted by extraction of a hydrous felsic melt (e.g. Clemens et al., 1986; Collins et al., 1982; Whalen et al., 1987). However, the latter process cannot account for some A-type granite characteristics, such as their high TiO_2/MgO and K_2O/Na_2O ratios (e.g. Creaser et al., 1991; Douce, 1997). Experimental results suggest that partial melting of a wide range of crustal rocks would leave refractory granulitic residues, which are depleted in alkalis relative to Al, and depleted in TiO_2 relative to MgO (Creaser et al., 1991; Douce, 1997). Remelting of these residues cannot produce granitic liquids with high $(Na_2O + K_2O)/Al_2O_3$ and TiO_2/MgO ratios that are characteristic of A-type granites. In order to produce granites containing chemical and isotope signatures of both mantle and crust, various models have been proposed suggesting fractionation of variously contaminated, mantle-derived alkali basalt (Bonin, 2007), mixing of crustal melts with OIB magma (Eby, 1990, 1992) and evolution of mantle-derived mafic and intermediate magmas (Bonin and Giret, 1990; Turner et al., 1992).

Zircon Hf model ages (T^{C}_{DM}) of the Baijuhuajian granites range from 733 to 968 Ma (Fig. 12), which may suggest that the Baijuhuajian granitic magma formed by partial melting of Neoproterozoic crust. Neoproterozoic mafic rocks crop out in South China and have been considered to be products of the break-up of the Rodinia super-continent (e.g. Li et al., 1999). However, the absence of inherited zircon with Neoproterozoic ages in the Baijuhuajian granite and its geochemical composition do not favour such an interpretation.

Mantle–crust interaction in the Baijuhuajian pluton is manifested by both its trace element and isotopic compositions. As discussed above, trace-element geochemistry of the Baijuhuajian granite suggests that the magma was enriched in mantle materials and that crustal assimilation was minor. For example, Nb and Ta contents are higher than I- and S-type granites, although there are wide ranges of

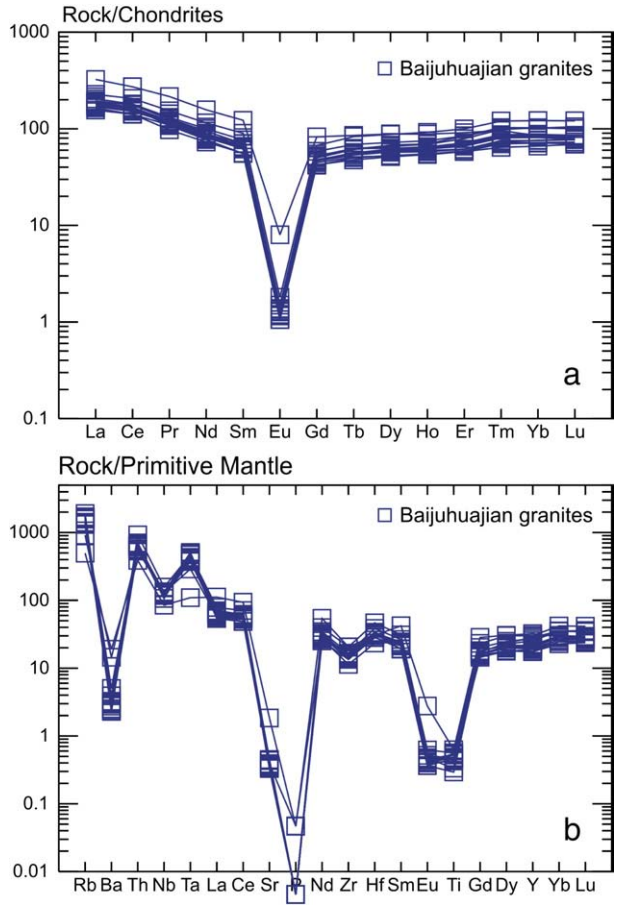

Fig. 9. (a) Chondrite-normalized REE diagram for the Baijuhuajian granite. Normalization values are from Sun and McDonough (1989). (b) Primitive mantle-normalized spider diagram for the Baijuhuajian granite. Normalization values are from Sun and McDonough (1989).

Nb and Ta concentrations in the samples (Nb = 61 to 112 ppm; Ta = 4 to 21 ppm). Its low Y/Nb ratio (0.9 to 2.4) and low Zr content also suggest little crustal contamination. These data indicate that felsic crustal material was not a major component in the magma source.

Zircon Hf isotope compositions are consistent with the aforementioned interpretation. Because Hf is partitioned more strongly into melts than Lu during partial melting (Belousova et al., 2006), the crust has lower $^{176}Lu/^{177}Hf$, and therefore lower $^{176}Hf/^{177}Hf$ ratios, than the mantle. During the generation of granitic magmas, input of juvenile mantle materials, either directly by mantle-derived mafic melts, or by remelting of juvenile mantle-derived mafic lower crust, can result in high $^{176}Hf/^{177}Hf$ ratios (i.e. $\varepsilon Hf(T)>0$). The $\varepsilon Hf(T)$ values of zircons from the Baijuhuajian granite vary from −0.52 to +4.24, implying a significant input of juvenile, mantle-derived materials during the magma generation.

Geochemical signatures of incompatible elements suggest an enriched mantle source for the Baijuhuajian pluton. Most of the Baijuhuajian samples plot in the OIB field in the Yb/Ta versus Y/Nb diagram (Fig. 13). We suggest that the Baijuhuajian magma was derived originally from the asthenospheric mantle and experienced extensive crystal fractionation and minor mixing with old crustal components. Geochemical data for Mesozoic granitoids along the coastal region of SE China and Taiwan suggest that mantle input played a significant role in the petrogenesis of the Mesozoic rocks in the region (e.g. Chen and Jahn, 1998; Jahn et al., 1990). The whole rock Nd isotopic composition of the Baijuhuajian granite indicates little evidence of crustal contamination, and the Nd model age (1.5 Ga) is similar to the model ages of other Mesozoic granites in SE China (e.g. Chen et al., 1999a; Chen and Jahn, 1998).

7.3. Regional extension and tectonic evolution between ca. 190 and 100 Ma

A-type granites generally form in extensional tectonic environments regardless of the origin of the magma source (e.g. Eby, 1992; Turner et al., 1992; Whalen et al., 1987). Mesozoic A-type granites in eastern South China attracted much attention because they have important tectonic implications. The Jurassic A-type granites only occur locally and most are distributed along the southern inland area of a E–W magmatic belt, e.g. the Nankunshan alkaline granites in Guangdong Province and Keshubei, Zhaibei and Beitou alkaline granites in Jiangxi Province (Chen et al., 1998; Fan and Chen, 2000; Li et al., 2007a,b; Liu et al., 2003). In contrast, the Cretaceous magmatism is dominated by high-potassium I-type and some A-type granites (Li, 2000; Zhou et al., 2006) that mainly occur along the coastal area in eastern Zhejiang and Fujian Provinces. The I- and S-type granites show a continuous age distribution and were emplaced in three periods i.e. 190–160 Ma in the west, 160–142 Ma in the central and 142–99 Ma in the east (Fig. 14) (Zhou et al., 2006). In contrast, only two distinct episodes of A-type granite, 190–160 Ma and ~100 Ma, have been reported in the literature. Prior to this study, the timing of extension in Zhejiang Province was considered to be ca. 100 Ma (e.g. Charvet et al., 1994; Gilder et al., 1991; Lapierre et al., 1997), but the Baijuhuajian pluton suggests that extension in SE China, could have started as early as ~125 Ma in the Province. The Suzhou granite pluton is another A-type granite in Jiangsu Province that was emplaced at 123 Ma (Charoy and Raimbault, 1994; Chen et al., 1993), but its tectonic

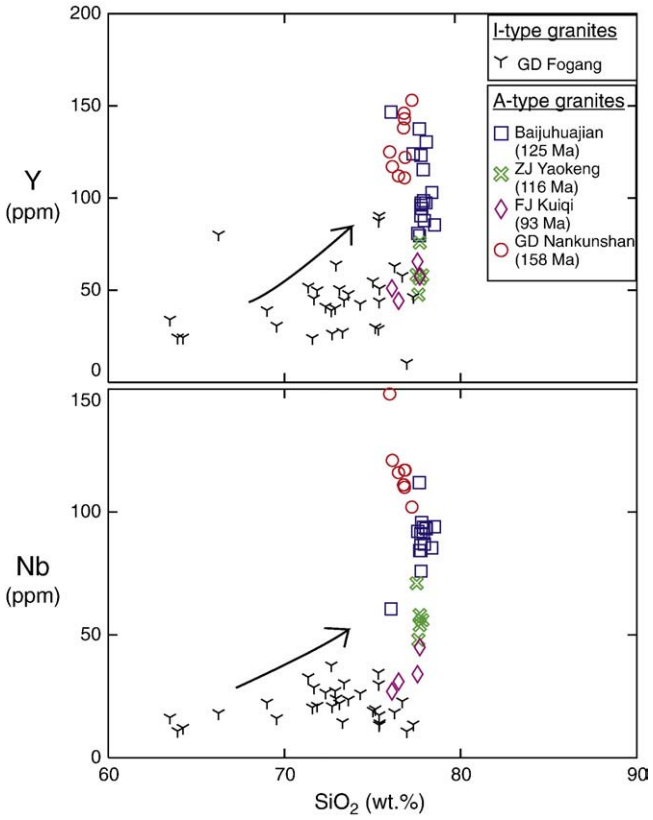

Fig. 10. Y versus SiO_2 and Nb versus SiO_2 diagrams for the Baijuhuajian granite In the Fogong I-type granite, Y and Nb show good correlations with SiO_2, but not in the A-type granite of the Baijuhuajian granite.

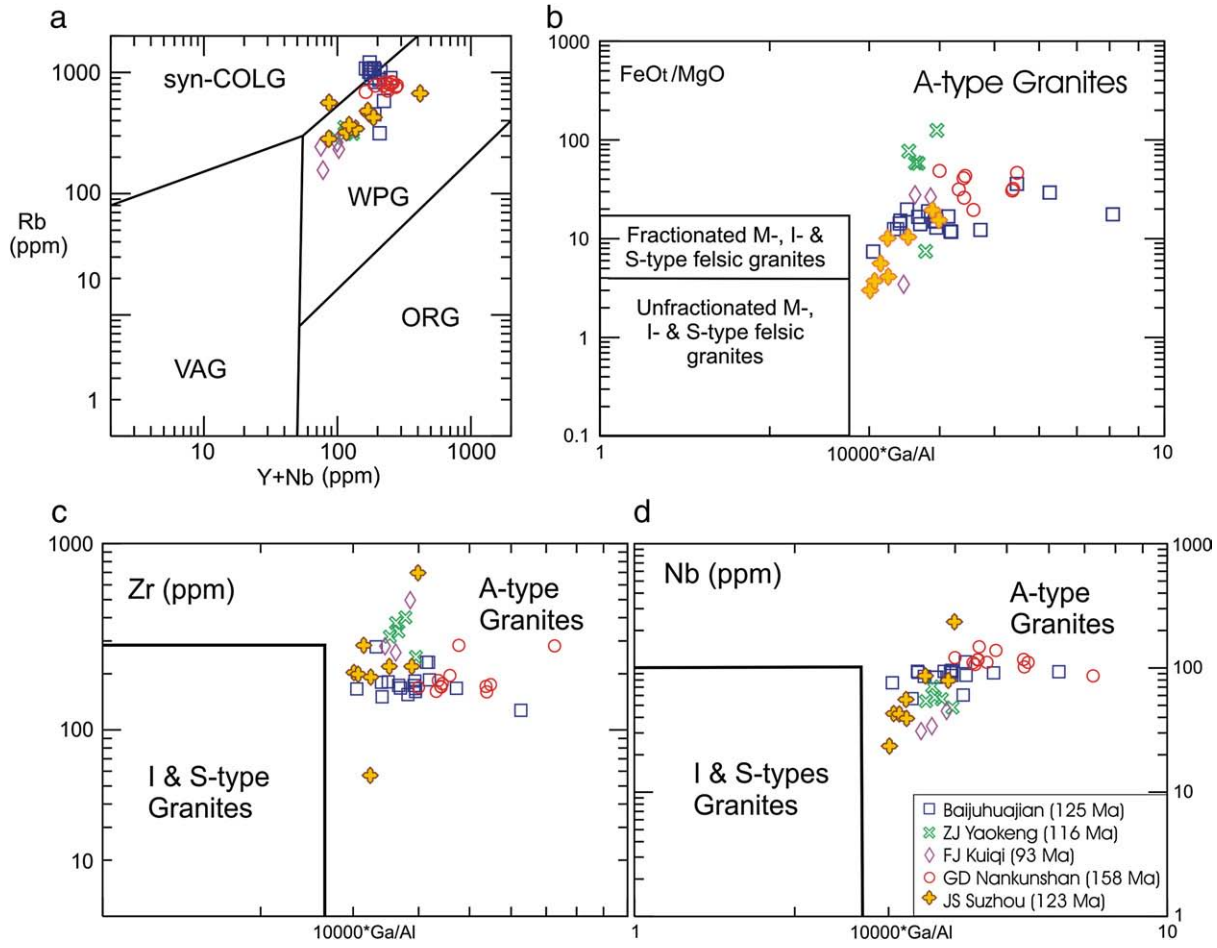

Fig. 11. (a) Discrimination diagrams for granites (Pearce et al., 1984). The Baijuhuajian granites plot in the field of WPG (= within-plate granite). (b) FeO_t/MgO vs 10,000 Ga/Al diagram (after Whalen et al., 1987). The Baijuhuajian granitic samples plot in the field of A-type granite. (c and d) Discrimination diagrams for granites (Whalen et al., 1987). Samples of the Baijuhuajian granite plot into the field of A-type granites. Other Mesozoic A-type granites are plotted for comparison: 116 Ma Yaokeng alkaline granite in Zhejiang Province (Qiu et al., 2000a), 93 Ma Kuiqi alkaline granite in Fujian Province (Martin et al., 1994), 158 Ma Nankunshan A-type granite in Guangdong Province (Li et al., 2007b; Liu et al., 2003) and 123 Ma Suzhou alkaline granite in Jiangsu Province (Charoy and Raimbault, 1994).

significance has generally been overlooked. Therefore, our data suggest two principal periods of extensional Mesozoic tectonism in South China. The first occurred in Guangdong and Jiangxi Provinces at 190 to 155 Ma, along the southern part of the magmatic belt. The second period of extension generated the Baijuhuajian and Suzhou granites near the central part of the magmatic belt at 125–123 Ma and the 100–90 Ma A-type granites were formed along the coastal area in eastern Zhejiang and Fujian Provinces. The regional extension, therefore, gradually migrated from inland to the coastal area. Despite an age gap between 125 and 155 Ma for the A-type granites, the above age pattern is broadly consistent with the distribution of other types of granitoids and volcanic rocks in southeastern China (Fig. 14). However, the paucity of A-type granitoids in southeast China, their regional distribution and their wide range of ages make it difficult identify any consistent pattern of regional extension.

It has been proposed that bimodal and alkaline granites with ages of 190 to 155 Ma in the internal region of SE China formed during a period of extension after the Indosinian Orogeny (e.g. Li et al., 2007a; Zhou, 2003). In contrast, Zhou (2003) proposed that the A-type granites emplaced at ca. 100 Ma in the coastal area reflect periods of rollback/back-arc extension of the Pacific Plate. In this case, interaction of the Eurasian and Pacific Plates played an important role in the tectonic and magmatic evolution of SE China. For example Li and Li (2007) proposed that the 189-Ma Keshubei A-type granite in Jiangxi Province marks the end of the Indosinian orogeny and the beginning of extension. According to their model, emplacement of the bimodal volcanic rocks, alkaline rocks and I- and A-type granites with ages of ca. 155 to 190 Ma in the central part of the magmatic belt was associated with slab foundering (Li and Li, 2007). This was supposedly followed by rollback of the subducting slab after ca. 150 Ma, which generated arc-related and bimodal magmatism, such as the high-potassium, I- and some A-type granites in the coastal region (e.g. Li and Li, 2007; Zhou and Li, 2000; Zhou et al., 2006).

We propose here a refined model that does not require regular periods of extension for A-type magmatism in SE China and the model is consistent with the relationship between the A-type granites and the dominant I-type rocks of the region. Based on the age distribution of the I-type magmatic rocks of this region, subduction continued more or less continuously throughout the Jurassic and Cretaceous. We suggest that the sparse A-type granites with similar or overlapping ages, represent irregular and episodic rollback of the paleo-Pacific Plate that led to localized extension in the upper plate. Like the dominant I-type igneous rocks, the A-type plutons generally become younger toward the coast in SE China but they do not define periods of regional extension over long periods of time. This model explains the appearance of volumetrically insignificant A-type granitoids in the region that have similar ages as the I-type granites and a similar younging trend toward the coast. It also explains why a series of localized extensional basins developed throughout the Cretaceous (e.g. Gilder et al., 1991; Shu et al., 2009; Zhou et al., 2006).

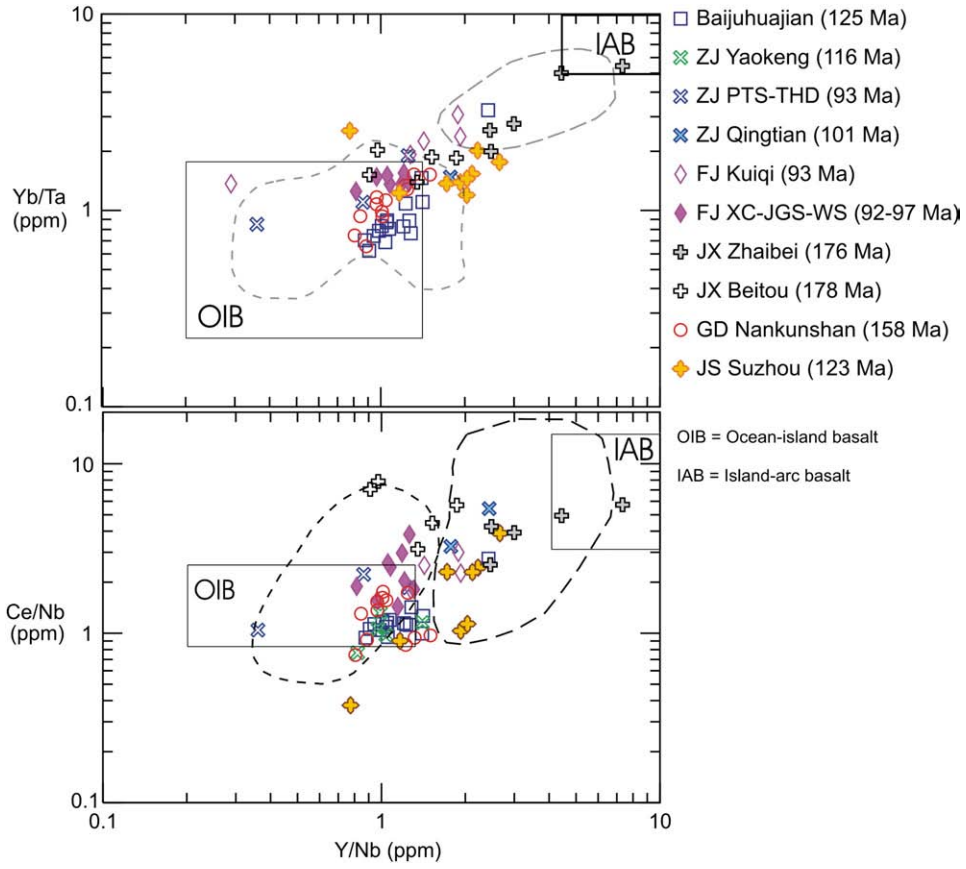

Fig. 12. Hf isotope evolution diagram. Data for Neoproterozoic intrusions in South China are from Zheng et al. (2007). Data for ca. 750–760-Ma Kangding granitoids in the Kangdian Rift of the South China Craton and the ~825-Ma granitoids from the Jiangnan Orogen are represented by dark grey squares and light squares, respectively (Zheng et al., 2007). The Baijuhuajian granitic magma may have been mixed with newly extracted basaltic magma from the asthenosphere during the Mesozoic with partial melting of old crustal material. The DM line denotes the evolution of depleted mantle with a present-day $^{176}Hf/^{177}Hf = 0.28325$ and $^{176}Lu/^{177}Hf = 0.0384$ (Griffin et al., 2000) and the corresponding lines of crustal extraction are calculated by assuming a $^{176}Lu/^{177}Hf$ ratio of 0.015 for the average continental crust.

Sun et al. (2007) noticed dramatic changes in the drift direction of the Pacific Plate at ~125–122 Ma (from southward to northwestward) and at ~100 Ma (from northwestward to northward) and correlated such changes with gold mineralization in eastern China. Here we see formation of A-type granites in South China in the period of 125–100 Ma. Whether the proposed rollback of the Pacific Plate was related to such changes in plate motion or was due to more local readjustments invites further investigation.

8. Conclusions

Geochemical data indicate that Baijuhuajian granite in the western Zhejiang Province is a metaluminous granite which exhibits typical geochemical signatures of A-type granites, such as high Fe* ($FeO_t/FeO_t + MgO$) and K_2O/Na_2O ratios, enrichment in incompatible elements (REE except Eu, Zr, Nb and Ta) and depletion in compatible elements in mafic silicates (Co, Sc, Cr, Ni) and feldspars (Ba, Sr and Eu).

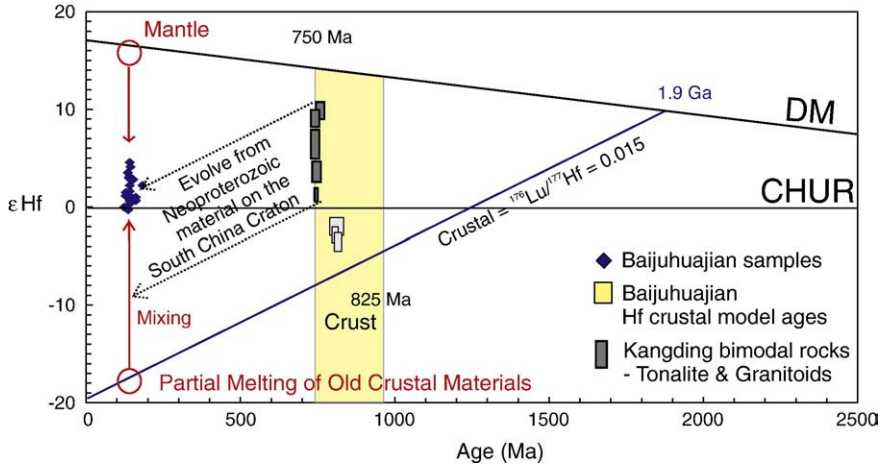

Fig. 13. (a) Yb/Ta versus Y/Nb and (b) Y/Nb versus Ce/Nb diagrams for the Baijuhuajian granite (Eby, 1992). OIB = ocean-island basalt; IAB = island-arc basalt. Fields with dashed lines represent A1- and A2-type granites of Eby (1990). For details of individual pluton refer to Table 1.

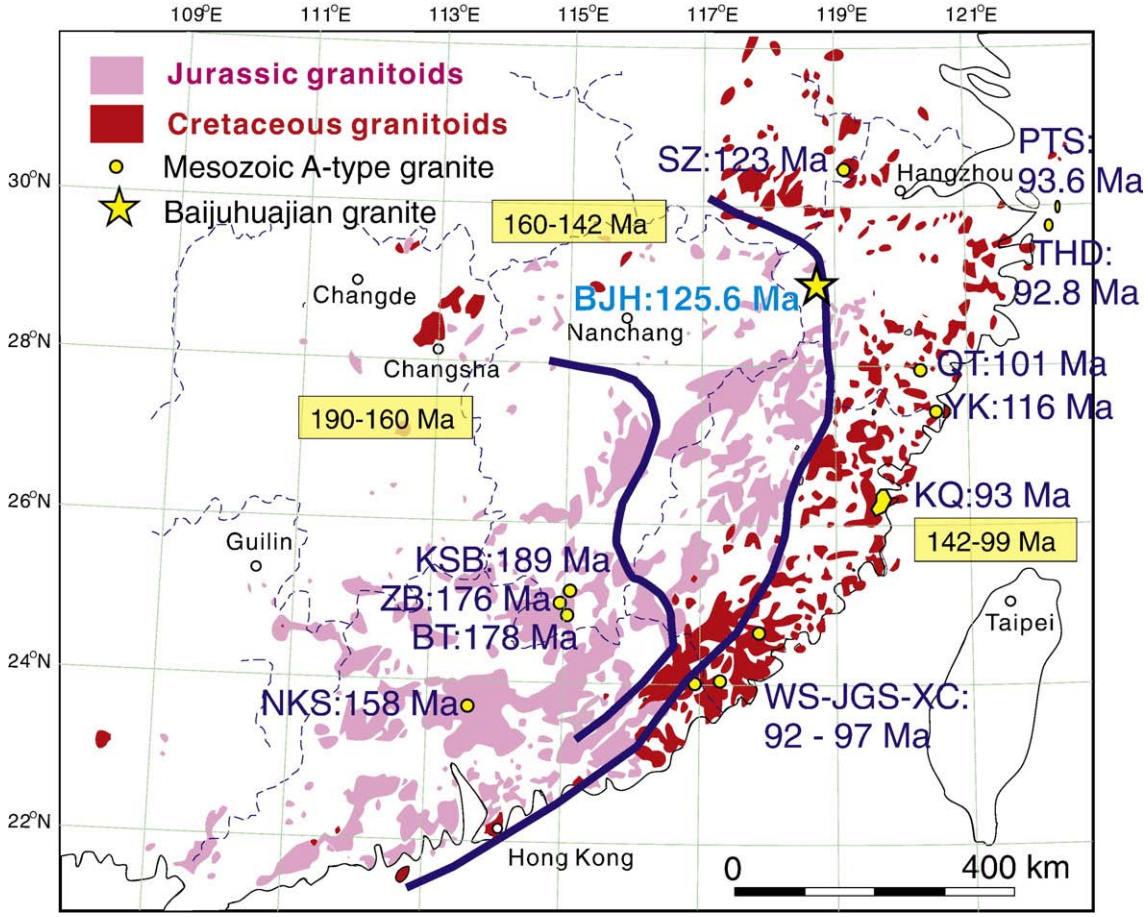

Fig. 14. Distribution of the Mesozoic A-type granites along the Mesozoic magmatic belt in southeastern China (modified after Zhou et al., 2006). The blue lines separate all types of the Late Mesozoic granites into three belts according to their ages, which are 190 to 160 Ma in the west, 160 to 142 Ma in the central and 142 to 99 Ma in the east (Zhou et al., 2006). The yellow star represents the Baijuhuajian granite. Other Mesozoic A-type granites are represented by yellow circles. For details of individual plutons refer to Table 1. (For interpretation of the references to color in this figure legend, the reader is referred to the web version of this article.)

Zircons from the Baijuhuajian granite have $\varepsilon Hf(T)$ values between −0.52 and +4.24, which suggest a predominantly mantle component in the magma source. The Baijuhuajian granite was emplaced at ~125 Ma, indicating the extension in the Fujian-Zhejiang Province started before the Early Cretaceous, rather than Late Cretaceous as previously suggested. Regional subduction generated a variety of granitoids throughout the Mesozoic, starting with 190 to 155 Ma plutons in the inland area (Jiangxi and Guangdong Provinces), through the middle area at 125 to 123 Ma (western Zhejiang, north to Jiangsu Provinces) and finally in the coastal area in Fujian and Zhejiang Provinces at 100 to 90 Ma. A-type granitoids with essentially contemporaneous ages were emplaced at ca. 190 to 155 Ma, and at ~125 to 100 Ma as a result of concomitant local extension due to a slab rollback and/or break-off of the subducting Pacific Plate.

Acknowledgements

The authors are grateful for Drs. Paul Robinson and Nelson Eby and an anonymous reviewer for their constructive reviews, which significantly improved the quality of this paper. Bernard Bonin is also thanked for his invaluable comments on an early version of this paper. We would like to thank Gregory Shellnutt and George S.-K. Ma for their scientific discussion and Xiao Fu, Lily Chiu, Liang Qi, Liewen Xie, Yueheng Yang and Jiangfeng Gao for their assistance with the geochemical analyses. This study was supported by the Research Grant Council of Hong Kong (HKU 7041/05P), the Chinese Ministry of Land and Resources (200811015), Knowledge Innovation Project of CAS (KZCX2-YW-Q08-3-6), and the CAS/SAFEA International Partnership Program for Creative Research Teams.

References

Ames, L., Zhou, G.Z., Xiong, B.C., 1996. Geochronology and isotopic character of ultrahigh-pressure metamorphism with implications for collision of the Sino-Korean and Yangtze cratons, central China. Tectonics 15 (2), 472–489.

Anderson, I.C., Frost, C.D., Frost, B.R., 2003. Petrogenesis of the Red Mountain pluton, Laramie anorthosite complex, Wyoming: implications for the origin of A-type granite. Precambrian Research 124 (2–4), 243–267.

Bao, Z., Zhao, Z., 2003. Geochemistry and tectonic setting of the Fugang aluminous A-type granite, Guangdong Province, China — a preliminary study. Geology - Geochemistry 31 (1), 52–61 (Chinese with English abstract).

Belousova, E.A., Griffin, W.L., O'Reilly, S.Y., 2006. Zircon crystal morphology, trace element signatures and Hf isotope composition as a tool for petrogenetic modelling: examples from eastern Australian granitoids. Journal of Petrology 47 (2), 329–353.

BGMRZP (Bureau of Geology and Mineral Resources of Zhejiang Province), 1989. Regional geology of Zhejiang Province. People's Republic of China, Ministry of Geology and Mineral Resources. Geological Memoirs, Series 1, No.11. Geological Publishing House, Beijing. 688 pp, (in Chinese).

Blichert-Toft, J., Albarede, F., 1997. The Lu–Hf isotope geochemistry of chondrites and the evolution of the mantle–crust system. Earth and Planetary Science Letters 148 (1–2), 243.

Bonin, B., 2007. A-type granites and related rocks: evolution of a concept, problems and prospects. Lithos 97 (1–2), 1–29.

Bonin, B., Giret, A., 1990. Plutonic alkaline series: Daly gap and intermediate compositions for liquids filling up crustal magma chambers. Schweizerisch und Petrographische Mitteilungen 70, 175–187.

Charoy, B., Raimbault, L., 1994. Zr-rich, Th-rich, and Ree-rich biotite differentiates in the A-type granite pluton of Suzhou (Eastern China) — the key role of fluorine. Journal of Petrology 35 (4), 919–962.

Charvet, J., Lapierre, H., Yu, Y.W., 1994. Geodynamic significance of the Mesozoic volcanism of southeastern China. Journal of Southeast Asian Earth Sciences 68, 387–396.

Chen, Q., Dickinson, W., 1986. Contrasting nature of petroliferous Mesozoic–Cenozoic Basins in eastern and western China. American Association Petroleum Geologists Bulletin 70, 263–275.
Chen, J.F., Jahn, B.M., 1998. Crustal evolution of southeastern China: Nd and Sr isotopic evidence. Tectonophysics 284, 101–133.
Chen, J.F., Foland, K.A., Liu, Y.M., 1993. Precise 40Ar/39Ar dating of the Suzhou composite granite. Acta Petrolei Sinica 9, 77–85 (in Chinese with English abstract).
Chen, P.R., Zhang, B.T., Kong, X.G., Cai, B.C., Ling, H.F., Ni, Q.S., 1998. Geochemical characteristics and tectonic implication of Zhaibei A-type granitic intrusives in South Jiangxi Province. Acta Petrologica Sinica 14 (3), 289–298 (in Chinese).
Chen, J.F., Guo, X., Tang, J., Zhou, T., 1999a. Nd isotopic model ages: implications of the growth of the continental crust of southeastern China. Journal of Nanjing University (Natural Sciences) 35 (6), 649–658 (in Chinese with English abstract).
Chen, P.R., Kong, X.G., Wang, Y.X., Ni, Q.S., Zhang, B.T., Ling, H.F., 1999b. Rb–Sr isotopic dating and significance of early Yanshanian bimodal volcanic-intrusive complex from southern Jiangxi Province, SE China. Geological Journal of China Universities 5, 378–382 (in Chinese with English abstract).
Chen, P.R., Kong, X.G., Ni, Q.S., Zhang, B.T., Liu, C.S., 1999c. Ascertainment and implication of the Early Yianshanian bimodal volcanic associations from south Jiangxi Province. Geological Review 45, 734–741 (in Chinese with English abstract).
Chu, N.C., Taylor, R.N., Chavagnac, V., Nesbitt, R.W., Boella, R.M., Milton, J.A., German, C.R., Bayon, G., Burton, K., 2002. Hf isotope ratio analysis using multi-collector inductively coupled plasma mass spectrometry: an evaluation of isobaric interference corrections. Journal of Analytical Atomic Spectrometry 17, 1567–1574.
Clemens, J.D., Holloway, J.R., White, A.J.R., 1986. Origin of an A-type granite: experimental constraints. American Mineralogist 71, 317–324.
Collins, W.J., Beams, S.D., White, A.J.R., Chappell, B.W., 1982. Nature and origin of A-type granites with particular reference to Southeastern Australia. Contributions to Mineralogy and Petrology 80, 189–200.
Creaser, R.A., Price, R.C., Wormald, R.J., 1991. A-type granites revisited: assessment of residual-source model. Geology 19, 163–166.
Douce, A.E.P., 1997. Generation of metaluminous A-type granites by low-pressure melting of calc-alkaline granitoids. Geology 25 (8), 743–746.
Eby, G.N., 1990. The A-type granitoids: a review of their occurrence and chemical characteristics and speculations on their petrogenesis. Lithos 26 (1–2), 115–134.
Eby, G.N., 1992. Chemical subdivision of the A-type granitoids: petrogenetic and tectonic implications. Geology 20, 641–644.
Fan, C.F., Chen, P.R., 2000. Geochemical characteristics and tectonic implication of Beitou A-type granitic intrusive in South Jiangxi Province. Geochimica 29 (4), 358–366 (in Chinese).
Gilder, S.A., Keller, G.R., Luo, M., Goodell, P.C., 1991. Timing and spatial distribution of rifting in China. Tectonophysics 197, 225–243.
Goldstein, S.L., Onions, R.K., Hamilton, P.J., 1984. A Sm–Nd isotopic study of atmospheric dusts and particulates from major river systems. Earth and Planetary Science Letters 70 (2), 221–236.
Greentree, M.R., Li, Z.-X., 2008. The oldest known rocks in south-western China: SHRIMP U–Pb magmatic crystallisation age and detrital provenance analysis of the Paleoproterozoic Dahongshan Group. Journal of Asian Earth Sciences 33 (5–6), 289–302.
Griffin, W.L., Pearson, N.J., Belousova, E., Jackson, S.E., van Achterbergh, E., O'Reilly, S.Y., Shee, S.R., 2000. The Hf isotope composition of cratonic mantle: LAM-MC-ICPMS analysis of zircon megacrysts in kimberlites. Geochimica Et Cosmochimica Acta 64 (1), 133–147.
Griffin, W.L., Wang, X.W., Jackson, S.E., Pearson, N.J., O'Reilly, S.Y., Xu, X., Zhou, X., 2002. Zircon chemistry and magma mixing, SE China: in-situ analysis of Hf isotopes, Tonglu and Pingtan igneous complexes. Lithos 61, 237–269.
Griffin, W.L., Belousova, E.A., Shee, S.R., Pearson, N.J., O'Reilly, S.Y., 2004. Archean crustal evolution in the northern Yilgarn Craton: U–Pb and Hf-isotope evidence from detrital zircons. Precambrian Research 131 (3–4), 231.
Holloway, N.H., 1982. North Palawan Block, Philippines — its relation to Asian Mainland and role in evolution of South China Sea. The American Association of Petroleum Geologists Bulletin 66, 1355–1383.
Hsü, K.J., Li, J.L., Chen, H.H., Pen, H.P., Senger, A.M.C., 1990. Tectonics of south China: key to understanding west Pacific geology. Tectonophysics 183, 9–39.
Hu, G.R., Chen, P.R., Yu, R.L., 2002. The characteristics of element geochemistry of Keshubei rock mass and its ore-forming significance. Geology and Prospecting 38 (6), 25–29 (Chinese with English abstract).
Jahn, B.M., Chen, P.Y., Yen, T.P., 1976. Rb–Sr ages of granitic rocks in southeastern China and their tectonic significance. Geological Society of America Bulletin 86, 763–776.
Jahn, B.M., Zhou, X.H., Li, J.L., 1990. Formation and tectonic evolution of southeastern China and Taiwan: isotopic and geochemical constraints. Tectonophysics 183, 145–160.
King, P.L., White, A.J.R., Chappell, W., Allen, C.M., 1997. Characterization and origin of aluminous A-type granites from the Lachlan Fold Belt, Southeastern Australia. Journal of Petrology 38 (3), 371–391.
Lapierre, H., Jahn, B.M., Charvet, J., Yu, Y.W., 1997. Mesozoic felsic arc magmatism and continental olivine tholeiites in Zhejiang Province and their relationship with the tectonic activity in southeastern China. Tectonophysics 274 (4), 321–338.
Li, X.H., 2000. Cretaceous magmatism and lithospheric extension in Southeast China. Journal of Asian Earth Sciences 18, 293–305.
Li, X.H., McCulloch, M.T., 1998. Geochemical characteristics of Cretaceous mafic dikes from northern Guangdong, SE China: age, origin and tectonic significance. Mantle Dynamics and Plate Interaction in East Asia, vol. 27. AGU Geodynamics, Washington, DC. 405–419 pp.
Li, Z.-X., Li, X.H., 2007. Formation of the 1300 km-wide intracontinental orogen and post-orogenic magmatic province in Mesozoic South China: a flat-slab subduction model. Geology 35, 179–182.
Li, Z.X., Li, X.-H., Kinny, P.D., Wang, J., 1999. The break-up of Rodinia: did it start with a mantle plume beneath South China? Earth and Planetary Science Letters 173, 171–181.
Li, X.-H., Li, Z.-X., Li, W.-X., Wang, Y., 2006. Initiation of the Indosinian Orogeny in South China: evidence for a Permian magmatic arc on Hainan Island. The Journal of Geology 114, 341–353.
Li, X.-H., Li, W.-X., Li, Z.-X., 2007a. On the genetic classification and tectonic implications of the Early Yanshanian granitoids in the Nanling Range, South China. Chinese Science Bulletin 52 (14), 1873–1885.
Li, X.-H., Li, Z.-X., Li, W.-X., Liu, Y., Yuan, C., Wei, G., Qi, C., 2007b. U-Pb zircon, geochemical and Sr–Nd–Hf isotopic constraints on age and origin of Jurassic I- and A-type granites from central Guangdong, SE China: a major igneous event in response to foundering of a subducted flat-slab? Lithos 96 (1–2), 186–204.
Li, Z.-X., Wartho, J.-A., Occhipinti, S., Zhang, C.-L., Li, X.-H., Wang, J., Bao, C., 2007c. Early history of the eastern Sibao Orogen (South China) during the assembly of Rodinia: new mica 40Ar/39Ar dating and SHRIMP U–Pb detrital zircon provenance constraints. Precambrian Research 159 (1–2), 79–94.
Liu, C.S., Chen, X.M., Wang, R.C., Hu, H., 2003. Origin of Nankunshan aluminous A-type granite, Longkou County, Guangdong Province. Acta Petrologica Et Mineralogica 22 (1), 1–10 (Chinese).
Loiselle, M.C., Wones, D.R., 1979. Characteristics of anorogenic granites. Geological Society of America Abstracts with Programs 11, 468.
Ludwig, K.R., 2003. Isoplot 3.00. Berkeley Geochronology Center, Special Publication, No. 4. 70 pp.
Machado, N., Simonetti, A., 2001. U–Pb dating and Hf isotopic composition of zircons by laser ablation-MC-ICP-MSA. In: Sylverster, P. (Ed.), Laser Ablation ICPMS in the Earth Sciences: Principles and Applications, Short Course, Mineralogical Association of Canada, vol. 29, pp. 121–146.
Martin, H., Bonin, B., Capdevia, R., Jahn, B.M., Lameyre, J., Wang, Y., 1994. The Kuiqi Peralkaline granitic complex (SE China): petrology and geochemistry. Journal of Petrology 35 (4), 983–1015.
Nelson, D.R., 1997. Compilation of SHRIMP U–Pb Zircon Geochronology Data, 1996: Geological Survey of Western Australia, Record 1997/2.
Norrish, K., Hutton, J.T., 1969. An accurate X-ray spectrographic method for the analysis of a wide range of geological samples. Geochimica et Cosmochimica Acta 33 (4), 431–453.
Ogg, J.G., Ogg, G., Gradstein, F.M., 2008. The Concise Geologic Time Scale. Cambridge University Press. 150 pp.
Pearce, J.A., Harris, N.B.W., Tindle, A.G., 1984. Trace element discrimination diagrams for the tectonic interpretation of granitic rocks. Journal of Petrology 25 (4), 956–983.
Peucat, J.J., Vidal, P., Bernard-Griffiths, J., Condie, K.C., 1988. Sr, Nd and Pb isotopic systematics in the Archaean low- to high-grade transition zone of southern India: syn accretions vs. post-accretion granulites. Journal of Geology 97, 537–550.
Pidgeon, R.T., Furfaro, D., Kennedy, A.K., Nemchin, A., van Bronswijk, W., Todt, W.A., 1994. Calibration of zircon standards for the Curtin SHRIMP II: Eighth International Conference on Geochronology, Cosmochronology and Isotope Geology, Berkeley, Abstract. 251.
Preccerillo, R., Taylor, S.R., 1976. Geochemistry of Eocene calc-alkaline volcanic rocks from characteristics of island arc basalts: implication for mantle sources. Chemical Geology 30, 227–256.
Qi, L., Hu, J., Conrad, G.D., 2000. Determination of trace elements in granites by inductively coupled plasma mass spectrometry. Talanta 51 (3), 507–513.
Qiao, G., 1988. Normalization of isotopic dilution analysis—a new program for isotope mass spectrometric analysis. Scientia Sinica 31, 1263–1268 (in Chinese with English abstract).
Qiu, J.S., Wang, D.Z., McInnes, B.I.A., 1999. Geochemistry and petrogenesis of the I- and A-type composite granite masses in the coastal area of Zhejiang and Fujian Province. Acta Petrologica Sinica 14 (2), 237–246 (in Chinese).
Qiu, J.S., Satoshi, K., Wang, D.Z., 2000a. Geochemical characteristics and genetic type of Yaokeng alkali granites in Cangnan Country, Zhejiang Province. Acta Petrologica Et Mineralogica 19 (2), 97–105 (in Chinese with English abstract).
Qiu, Y.M., Gao, S., McNaughton, N., Groves, D.I., Ling, W.L., 2000b. First evidence of >3.2 Ga continental crust in the Yangtze craton of South China and its implications for Archean crustal evolution and Phanerozoic tectonics. Geology 28, 11–14.
Scherer, E., Munker, C., Mezger, K., 2001. Calibration of the lutetium–hafnium clock. Science 293, 683–687.
Shu, L.S., Zhou, X.M., Deng, P., Wang, B., Jiang, S.Y., Yu, J.H., Zhao, X.X., 2009. Mesozoic tectonic evolution of the Southeast China Block: new insights from basin analysis. Journal of Asian Earth Sciences 34 (3), 376–391.
Smith, D.R., Noblett, J., Wobus, R.A., Unruh, D., Douglass, J., Beane, R., Davis, C., Goldman, S., Kay, G., Gustavson, B., 1999. Petrology and geochemistry of late-stage intrusions of the A-type, mid-Proterozoic Pikes Peak batholith (Central Colorado, USA): implications for petrogenetic models. Precambrian Research 98 (3–4), 271–305.
Steiger, R.H., Jäger, E., 1977. Subcommission on geochronology: convention on the use of decay constants in geo- and cosmochronology. Earth and Planetary Science Letters 36, 359–362.
Streckeisen, A., Le Maitre, R.W., 1979. A chemical approximation to the modal QAPF classification of igneous rocks. Neues Jahrbuch für Mineralogie, Abhandlungen 136, 169–206.
Sun, S.S., McDonough, W.F., 1989. Chemical and isotopic systematics of oceanic basalts: implications for mantle composition and processes. In: Saunders, A.D., Norry, M.J. (Eds.), Magmatism in the ocean basalts. Geological Society Special Publication, pp. 313–345.
Sun, W., Ding, X., Hu, Y.-H., Li, X.-H., 2007. The golden transformation of the Cretaceous plate subduction in the west Pacific. Earth and Planetary Science Letters 262 (3–4), 533–542.
Turner, S.P., Foden, J.D., Morrison, R.S., 1992. Derivation of some A-Type magmas by fractionation of basaltic magma — an example from the Padthaway Ridge, South Australia. Lithos 28 (2), 151–179.

Wang, Y.J., Fan, W.M., Peng, T.P., Guo, F., 2004. Early Mesozoic OIB-type alkaline basalts in central Jiangxi Province and its tectonic implication. Geochimica 33, 109–117 (in Chinese with Englsih abstract).
Wang, Y.J., Fan, W.M., Peng, T.P., Guo, F., 2005. Elemental and Sr–Nd isotopic systematics of the early Mesozoic volcanic sequence in southern Jiangxi Province, South China: petrogenesis and tectonic implications. International Journal of Earth Sciences 94, 53–65.
Wang, X.L., Zhou, J.C., Qiu, J.S., Zhang, W.L., Liu, X.M., Zhang, G.L., 2006. LA-ICP-MS U–Pb zircon geochronology of the Neoproterozoic igneous rocks from Northern Guangxi, South China: Implications for tectonic evolution. Precambrian Research 145 (1–2), 111–130.
Wei, G.J., Liu, Y., Tu, X.L., Liang, X.R., Li, X.H., 2004. Separation of Sr, Sm and Nd in mineral and rock samples using selective specific resins. Rock and Mineral Analysis 23 (1), 11–14 (in Chinese with English abstract).
Whalen, J.B., Currie, K.L., Chappell, B.W., 1987. A-type granites: geochemical characteristics, discrimination and petrogenesis. Contributions to Mineralogy and Petrology 95 (4), 407.
Wu, F.Y., Yang, Y.H., Xie, L.W., Yang, J.H., Xu, P., 2006. Hf isotopic compositions of the standard zircons and baddeleyites used in U–Pb geochronology. Chemical Geology 234 (1–2), 105–126.
Xu, J., Zhu, G., Tong, W.X., Gui, K.R., Liu, Q., 1987. Formation and evolution of the Tancheng-Lujiang wrench fault system: a major shear system to the northwest of the Pacific Ocean. Tectonophysics 134, 273–310.
Xu, X., O'Reilly, S.Y., Griffin, W.L., Wang, X., Pearson, N.J., He, Z., 2007. The crust of Cathaysia: age, assembly and reworking of two terranes. Precambrian Research 158 (1–2), 51–78.
Ye, M.-F., Li, X.-H., Li, W.-X., Liu, Y., Li, Z.-X., 2007. SHRIMP zircon U-Pb geochronological and whole-rock geochemical evidence for an early Neoproterozoic Sibaoan magmatic arc along the southeastern margin of the Yangtze Block. Gondwana Research 12 (1–2), 144–156.
Zhang, X., Wang, J., Shen, B., 1988. A study on A-type granites in Suzhou, China. Chinese Journal of Geochemistry 7 (1), 29–45.
Zhao, G., Cawood, P.A., 1999. Tectonothermal evolution of the Mayuan Assemblage in the Cathaysia Block: implications for Neoproterozoic collision-related assembly of the South China Craton. American Journal of Science 299, 309–339.
Zheng, J.P., Griffin, W.L., O'Reilly, S.Y., Zhang, M., Pearson, N., Pan, Y.M., 2006. Widespread Archean basement beneath the Yangtze craton. Geology 34 (6), 417–420.
Zheng, Y.-F., Zhang, S.-B., Zhao, Z.-F., Wu, Y.-B., Li, X., Li, Z., Wu, F.-Y., 2007. Contrasting zircon Hf and O isotopes in the two episodes of Neoproterozoic granitoids in South China: Implications for growth and reworking of continental crust. Lithos 96 (1–2), 127–150.
Zhou, X.-M., 2003. My thinking about granite geneses of South China. Geological Journal of China Universities 9 (4), 556–565 (in Chinese).
Zhou, X.H., Li, W.X., 2000. Origin of Late Mesozoic igneous rocks in Southeastern China: implications for lithosphere subduction and underplating of mafic magmas. Tectonophysics 326, 269–287.
Zhou, X.M., Sun, T., Shen, W.Z., Shu, L.S., Niu, Y.L., 2006. Petrogenesis of Mesozoic granitoids and volcanic rocks in South China: a response to tectonic evolution. Episodes 29 (1), 26–33.